## Network analysis

We assigned selected genetic variants to a single protein-coding gene according to the following hierarchy: coding>intronic>5′UTR>3′UTR>near gene (within 2 kb to 5′ or 0.5 kb to 3′ of a gene)>intergenic. If a selected variant mapped an intergenic region, we sought literature of fine-mapping studies or GWAS of RA and other autoimmune diseases showing evidence of association of variants in higher levels of the hierarchy.

The physical PPI network was constructed using the HPRD database [75,76]. In PPI networks, vertices are proteins and edges represent a physical interaction between two proteins. We projected the RA-associated genes onto the constructed PPI network and candidate genes were then ranked based on the global distance to the RA-associated genes within the PPI network by using random walk with restart (RWR) algorithm [77]. The RWR algorithm is a powerful tool to measure proximity between vertices on complex network.

In a random walk, starting at some initial 'seed' vertices (i.e., proteins encoded by the RA-associated genes), we chose at random an edge that is attached to the current vertex and move along the chosen edge to the linked vertex, and iterate many steps. In the RWR, at each step of the walk we return to the initial seed vertices with the restart probability, $r$. All vertices are ranked by the number of times that the walker visits to corresponding vertices in the process. The outline is described below.

The adjacency matrix $\mathbf{A}$ of the PPI network is the matrix with elements $A_{ij}$ as follows: $A_{ij} = \begin{cases} 1 & \text{if there is an edge between vertices } i \text{ and } j \\ 0 & \text{otherwise} \end{cases}$. We define the transition probability matrix $\mathbf{M}$ so that the transition probability $M_{ij}$ from protein $i$ to protein $j$ is: $M_{ij} = A_{ij} \Big/ \sum_j A_{ij}$. Let $\mathbf{p}^{(t)}$ be a vector whose $i$-th element holds the probability of a random walker being at vertex $i$ at step $t$ and $\mathbf{p}^{(0)}$ be the initial-state probability vector, the probability vector at the step $t+1$ is as follows:

$$\mathbf{p}^{(t+1)} = (1-r)\mathbf{M}\mathbf{p}^{(t)} + r\mathbf{p}^{(0)}.$$

In this study, $\mathbf{p}^{(0)}$ was defined as the vector with elements: $p_i^{(0)} = \begin{cases} 1/\text{number of RA-associated genes} & \text{if vertex } i \text{ is RA-associated gene} \\ 0 & \text{otherwise} \end{cases}$ The restart probability $r$ was set to be 0.5. We considered the random walker reached a steady-state when the difference between $\mathbf{p}^{(t+1)}$ and $\mathbf{p}^{(t)}$ (measured by the L1 norm) reached $10^{-10}$. All the genes in the PPI network were ranked according to the corresponding values in the steady-state probability vector $\mathbf{p}^{(\infty)}$.

The predictive ability of the network-guided prioritization of genes was tested using leave-one-out cross-validation by omitting each RA-associated gene in turn from initial 'seed' vertices and performing the RWR algorithm for the purpose of its own evaluation. The ROC curve was drawn by plotting the TPR versus the FPR for all genes ranked above a sliding ranking threshold.

We define RA-associated network as a subnetwork in which vertices are the RA-associated genes and genes ranked in the top 100 by the RWR algorithm and edges are physical interactions between their products. Functional modules are then explored in the RA-associated network. The overlapping and hierarchical clusters were detected by using the EAGLE algorithm [84]. The functional annotation for the retrieved clusters was performed by using DAVID [85,86]. We set 9,521 genes on the PPI network from HPRD as the background in enrichment analysis.

## Supporting Information

**Figure S1 Flowchart detailing the exclusion and inclusion criteria and the number of studies excluded and included at each step of the electronic database searches.** A) PubMed, and B) NHGRI GWAS catalog.
(TIF)

**Figure S2 RA-associated network comprising known RA-associated genes and genes ranked in the top 50 by the RWR algorithm and edges are physical interactions between their products.** Nodes are color coded by hierarchical clusters detected by the EAGLE algorithm: CL1, red; CL2; cyan, and CL3, yellow. Overlapped regions between CL1 and CL2 are rendered in green. Node size is based on the ranking in the RWR algorithm.
(TIF)

**Figure S3 RA-associated network comprising known RA-associated genes and genes ranked in the top 150 by the RWR algorithm and edges are physical interactions between their products.** Nodes are color coded by hierarchical clusters detected by the EAGLE algorithm: CL1, red; CL2; cyan, CL3, yellow; and CL4, orange. Overlapped regions between CL1 and CL2, CL1 and CL4, and CL2 and CL4 are rendered in green, pink, and purple, respectively. Node size is based on the ranking in the RWR algorithm.
(TIF)

**Figure S4 Re-consideration on RA-associated network.** The RWR algorithm was re-examined by adding recently discovered 4 genes (*AIRE*, *CD247*, *UBASH3A*, and *ATXN2*). Nodes are color coded by hierarchical clusters detected by the EAGLE algorithm: CL1, red; CL2; cyan, and CL3, yellow. Overlapped regions between CL1 and CL2 are rendered in green. Node size is based on the ranking in the RWR algorithm.
(TIFF)

**Table S1 Result of ratings for 87 abstracts retrieved from PubMed.** The scoring was conducted by independent two authors (Hirofumi Nakaoka and Tailin Cui), which is color-coded in green and blue, respectively. Any disagreement between the two researchers was accommodated by Atsushi Tajima. The final decision is rendered in red.
(DOC)

**Table S2 Result of rating for 54 full-text articles.**
(DOC)

**Table S3 Result of screening of extracted data from 51 full-text articles.**
(DOC)

**Table S4 Re-analysis of meta-analyses addressing genetic associations with RA risk.**
(DOC)

**Table S5 Assignment of a single gene to genetic variants associated with RA and the allele frequencies in European and Japanese.**
(DOC)

**Table S6 Ethnic group-specific analysis of published meta-analyses of genetic associations with RA risk.** The SNPs in which the heterogeneity in the ORs between European and East Asian populations are significant are highlighted in yellow.
(DOC)

**Table S7 Genotype counts for six *HLA-DRB1* alleles and 15 SNPs.**
(DOC)

**Table S8 Association analysis of RF and anti-CCP positive RA patients versus control subjects with selected genetic variants.**
(DOC)

**Table S9 GO and KEGG annotations for three clusters in RA-associated network comprising RA-associated genes and genes ranked in the top 50 by the RWR algorithm.**
(DOC)

**Table S10 GO and KEGG annotations for three clusters in RA-associated network comprising RA-associated genes and genes ranked in the top 150 by the RWR algorithm.**
(DOC)

**Table S11 Re-consideration on RA-associated network.** The RWR algorithm was re-examined by adding recently discovered 4 genes (*AIRE*, *CD247*, *UBASH3A*, and *ATXN2*). GO and KEGG annotations for three clusters in RA-associated network comprising RA-associated genes and genes ranked in the top 100 by the RWR algorithm.
(DOC)

**Text S1 Supplementary methods.**
(DOC)

## Acknowledgments

We thank all the study participants and supporting medical staffs for making this study possible. We are grateful to Keiko Asami and Hiromi Moriya for their contribution to sample data collection. We wish to thank Hiromi Kamura, Kaori Fukushima, Ryota Sugimoto and Hideki Hayashi for their technical support.

## Author Contributions

Conceived and designed the experiments: HN AT HI II. Performed the experiments: AO SM KK. Analyzed the data: HN TC AT. Contributed reagents/materials/analysis tools: YH SS YS HI. Wrote the paper: HN AT II.

## References

1. Manolio TA, Brooks LD, Collins FS (2008) A HapMap harvest of insights into the genetics of common disease. J Clin Invest 118(5): 1590–1605.
2. Hirschhorn JN (2009) Genomewide association studies–illuminating biologic pathways. N Engl J Med 360(17): 1699–1701. 10.1056/NEJMp0808934.
3. Yang Q, Khoury MJ, Botto L, Friedman JM, Flanders WD (2003) Improving the prediction of complex diseases by testing for multiple disease-susceptibility genes. Am J Hum Genet 72(3): 636–649. 10.1086/367923.
4. Gulcher J, Stefansson K (2010) Genetic risk information for common diseases may indeed be already useful for prevention and early detection. Eur J Clin Invest 40(1): 56–63. 10.1111/j.1365-2362.2009.02233.x.
5. Janssens AC, van Duijn CM (2008) Genome-based prediction of common diseases: Advances and prospects. Hum Mol Genet 17(R2): R166–73. 10.1093/hmg/ddn250.
6. Kraft P, Hunter DJ (2009) Genetic risk prediction–are we there yet? N Engl J Med 360(17): 1701–1703. 10.1056/NEJMp0810107.
7. Pharoah PD, Antoniou AC, Easton DF, Ponder BA (2008) Polygenes, risk prediction, and targeted prevention of breast cancer. N Engl J Med 358(26): 2796–2803. 10.1056/NEJMsa0708739.
8. Ransohoff DF, Khoury MJ (2010) Personal genomics: Information can be harmful. Eur J Clin Invest 40(1): 64–68. 10.1111/j.1365-2362.2009.02232.x.
9. Manolio TA, Collins FS, Cox NJ, Goldstein DB, Hindorff LA, et al. (2009) Finding the missing heritability of complex diseases. Nature 461(7265): 747–753. 10.1038/nature08494.
10. Goldstein DB (2009) Common genetic variation and human traits. N Engl J Med 360(17): 1696–1698. 10.1056/NEJMp0806284.
11. Cohen JC, Kiss RS, Pertsemlidis A, Marcel YL, McPherson R, et al. (2004) Multiple rare alleles contribute to low plasma levels of HDL cholesterol. Science 305(5685): 869–872. 10.1126/science.1099870.
12. Ji W, Foo JN, O'Roak BJ, Zhao H, Larson MG, et al. (2008) Rare independent mutations in renal salt handling genes contribute to blood pressure variation. Nat Genet 40(5): 592–599. 10.1038/ng.118.
13. Nejentsev S, Walker N, Riches D, Egholm M, Todd JA (2009) Rare variants of IFIH1, a gene implicated in antiviral responses, protect against type 1 diabetes. Science 324(5925): 387–389. 10.1126/science.1167728.
14. McCarthy MI (2009) Exploring the unknown: Assumptions about allelic architecture and strategies for susceptibility variant discovery. Genome Med 1(7): 66. 10.1186/gm66.
15. Janssens AC, Gwinn M, Bradley LA, Oostra BA, van Duijn CM, et al. (2008) A critical appraisal of the scientific basis of commercial genomic profiles used to assess health risks and personalize health interventions. Am J Hum Genet 82(3): 593–599. 10.1016/j.ajhg.2007.12.020.
16. Cook NR, Ridker PM (2009) Advances in measuring the effect of individual predictors of cardiovascular risk: The role of reclassification measures. Ann Intern Med 150(11): 795–802.
17. Janssens AC, van Duijn CM (2009) Genome-based prediction of common diseases: Methodological considerations for future research. Genome Med 1(2): 20. 10.1186/gm20.
18. NCI-NHGRI Working Group on Replication in Association Studies, Chanock SJ, Manolio T, Boehnke M, Boerwinkle E, et al. (2007) Replicating genotype-phenotype associations. Nature 447(7145): 655–660.
19. Khoury MJ, Gwinn M, Ioannidis JP (2010) The emergence of translational epidemiology: From scientific discovery to population health impact. Am J Epidemiol 172(5): 517–524. 10.1093/aje/kwq211.
20. Nakaoka H, Inoue I (2009) Meta-analysis of genetic association studies: Methodologies, between-study heterogeneity and winner's curse. J Hum Genet 54(11): 615–623. 10.1038/jhg.2009.95.
21. Nadeau JH, Dudley AM (2011) Genetics. systems genetics. Science 331(6020): 1015–1016. 10.1126/science.1203869.
22. Vidal M, Cusick ME, Barabasi AL (2011) Interactome networks and human disease. Cell 144(6): 986–998. 10.1016/j.cell.2011.02.016.
23. Klareskog L, Catrina AI, Paget S (2009) Rheumatoid arthritis. Lancet 373(9664): 659–672. 10.1016/S0140-6736(09)60008-8.
24. Orozco G, Barton A (2010) Update on the genetic risk factors for rheumatoid arthritis. Expert Rev Clin Immunol 6(1): 61–75.
25. Plenge RM (2009) Recent progress in rheumatoid arthritis genetics: One step towards improved patient care. Curr Opin Rheumatol 21(3): 262–271. 10.1097/BOR.0b013e32832a2e2d.
26. van der Helm-van Mil AH, Huizinga TW (2008) Advances in the genetics of rheumatoid arthritis point to subclassification into distinct disease subsets. Arthritis Res Ther 10(2): 205. 10.1186/ar2384.
27. Begovich AB, Chang M, Schrodi SJ (2007) Meta-analysis evidence of a differential risk of the FCRL3 -169T→C polymorphism in white and east asian rheumatoid arthritis patients. Arthritis Rheum 56(9): 3168–3171. 10.1002/art.22857.
28. Burr ML, Naseem H, Hinks A, Eyre S, Gibbons LJ, et al. (2010) PADI4 genotype is not associated with rheumatoid arthritis in a large UK caucasian population. Ann Rheum Dis 69(4): 666–670. 10.1136/ard.2009.111294.
29. Daha NA, Kurreeman FA, Marques RB, Stoeken-Rijsbergen G, Verduijn W, et al. (2009) Confirmation of STAT4, IL2/IL21, and CTLA4 polymorphisms in rheumatoid arthritis. Arthritis Rheum 60(5): 1255–1260. 10.1002/art.24503.
30. Dieguez-Gonzalez R, Calaza M, Perez-Pampin E, de la Serna AR, Fernandez-Gutierrez B, et al. (2008) Association of interferon regulatory factor 5 haplotypes, similar to that found in systemic lupus erythematosus, in a large subgroup of patients with rheumatoid arthritis. Arthritis Rheum 58(5): 1264–1274. 10.1002/art.23426.
31. Han S, Li Y, Mao Y, Xie Y (2005) Meta-analysis of the association of CTLA-4 exon-1 +49A/G polymorphism with rheumatoid arthritis. Hum Genet 118(1): 123–132. 10.1007/s00439-005-0033-9.
32. Han SW, Lee WK, Kwon KT, Lee BK, Nam EJ, et al. (2009) Association of polymorphisms in interferon regulatory factor 5 gene with rheumatoid arthritis: A metaanalysis. J Rheumatol 36(4): 693–697. 10.3899/jrheum.081054.
33. Harrison P, Pointon JJ, Chapman K, Roddam A, Wordsworth BP (2008) Interleukin-1 promoter region polymorphism role in rheumatoid arthritis: A meta-analysis of IL-1B-511A/G variant reveals association with rheumatoid arthritis. Rheumatology (Oxford) 47(12): 1768–1770. 10.1093/rheumatology/ken374.
34. Iwamoto T, Ikari K, Nakamura T, Kuwahara M, Toyama Y, et al. (2006) Association between PADI4 and rheumatoid arthritis: A meta-analysis. Rheumatology (Oxford) 45(7): 804–807. 10.1093/rheumatology/kel023.
35. Ji JD, Lee WJ, Kong KA, Woo JH, Choi SJ, et al. (2010) Association of STAT4 polymorphism with rheumatoid arthritis and systemic lupus erythematosus: A meta-analysis. Mol Biol Rep 37(1): 141–147. 10.1007/s11033-009-9553-z.
36. Lee YH, Ji JD, Song GG (2009) Association between interleukin 1 polymorphisms and rheumatoid arthritis susceptibility: A metaanalysis. J Rheumatol 36(1): 12–15. 10.3899/jrheum.080450.

37. Lee YH, Ji JD, Song GG (2008) Associations between FCGR3A polymorphisms and susceptibility to rheumatoid arthritis: A metaanalysis. J Rheumatol 35(11): 2129–2135.
38. Lee YH, Ji JD, Song GG (2007) Tumor necrosis factor-alpha promoter -308 A/G polymorphism and rheumatoid arthritis susceptibility: A metaanalysis. J Rheumatol 34(1): 43–49.
39. Lee YH, Rho YH, Choi SJ, Ji JD, Song GG (2007) PADI4 polymorphisms and rheumatoid arthritis susceptibility: A meta-analysis. Rheumatol Int 27(9): 827–833. 10.1007/s00296-007-0320-y.
40. Lee YH, Rho YH, Choi SJ, Ji JD, Song GG, et al. (2007) The PTPN22 C1858T functional polymorphism and autoimmune diseases–a meta-analysis. Rheumatology (Oxford) 46(1): 49–56. 10.1093/rheumatology/kel170.
41. Lee YH, Woo JH, Choi SJ, Ji JD, Song GG (2010) Fc receptor-like 3 -169 C/T polymorphism and RA susceptibility: A meta-analysis. Rheumatol Int 30(7): 947–953. 10.1007/s00296-009-1082-5.
42. Lee YH, Woo JH, Choi SJ, Ji JD, Song GG (2010) Association between the rs7574865 polymorphism of STAT4 and rheumatoid arthritis: A meta-analysis. Rheumatol Int 30(5): 661–666. 10.1007/s00296-009-1051-z.
43. Lei C, Dongqing Z, Yeqing S, Oaks MK, Lishan C, et al. (2005) Association of the CTLA-4 gene with rheumatoid arthritis in chinese han population. Eur J Hum Genet 13(7): 823–828. 10.1038/sj.ejhg.5201423.
44. Lindner E, Nordang GB, Melum E, Flato B, Selvaag AM, et al. (2007) Lack of association between the chemokine receptor 5 polymorphism CCR5delta32 in rheumatoid arthritis and juvenile idiopathic arthritis. BMC Med Genet 8: 33. 10.1186/1471-2350-8-33.
45. Okada Y, Mori M, Yamada R, Suzuki A, Kobayashi K, et al. (2008) SLC22A4 polymorphism and rheumatoid arthritis susceptibility: A replication study in a japanese population and a metaanalysis. J Rheumatol 35(9): 1723–1728.
46. Orozco G, Alizadeh BZ, Delgado-Vega AM, Gonzalez-Gay MA, Balsa A, et al. (2008) Association of STAT4 with rheumatoid arthritis: A replication study in three european populations. Arthritis Rheum 58(7): 1974–1980. 10.1002/art.23549.
47. Orozco G, Eyre S, Hinks A, Ke X, Wellcome Trust Case Control consortium YEAR Consortium, et al. (2010) Association of CD40 with rheumatoid arthritis confirmed in a large UK case-control study. Ann Rheum Dis 69(5): 813–816. 10.1136/ard.2009.109579.
48. Patsopoulos NA, Ioannidis JP (2010) Susceptibility variants for rheumatoid arthritis in the TRAF1-C5 and 6q23 loci: A meta-analysis. Ann Rheum Dis 69(3): 561–566. 10.1136/ard.2009.109447.
49. Plant D, Barton A, Thomson W, Ke X, Eyre S, et al. (2009) A re-evaluation of three putative functional single nucleotide polymorphisms in rheumatoid arthritis. Ann Rheum Dis 68(8): 1373–1375. 10.1136/ard.2008.103572.
50. Plenge RM, Padyukov L, Remmers EF, Purcell S, Lee AT, et al. (2005) Replication of putative candidate-gene associations with rheumatoid arthritis in >4,000 samples from north america and sweden: Association of susceptibility with PTPN22, CTLA4, and PADI4. Am J Hum Genet 77(6): 1044–1060. 10.1086/498651.
51. Prahalad S (2006) Negative association between the chemokine receptor CCR5-Delta32 polymorphism and rheumatoid arthritis: A meta-analysis. Genes Immun 7(3): 264–268. 10.1038/sj.gene.6364298.
52. Raychaudhuri S, Remmers EF, Lee AT, Hackett R, Guiducci C, et al. (2008) Common variants at CD40 and other loci confer risk of rheumatoid arthritis. Nat Genet 40(10): 1216–1223. 10.1038/ng.233.
53. Suarez-Gestal M, Calaza M, Dieguez-Gonzalez R, Perez-Pampin E, Pablos JL, et al. (2009) Rheumatoid arthritis does not share most of the newly identified systemic lupus erythematosus genetic factors. Arthritis Rheum 60(9): 2558–2564. 10.1002/art.24748.
54. Takata Y, Inoue H, Sato A, Tsugawa K, Miyatake K, et al. (2008) Replication of reported genetic associations of PADI4, FCRL3, SLC22A4 and RUNX1 genes with rheumatoid arthritis: Results of an independent japanese population and evidence from meta-analysis of east asian studies. J Hum Genet 53(2): 163–173. 10.1007/s10038-007-0232-4.
55. Wheeler J, McHale M, Jackson V, Penny M (2007) Assessing theoretical risk and benefit suggested by genetic association studies of CCR5: Experience in a drug development programme for maraviroc. Antivir Ther 12(2): 233–245.
56. Barnetche T, Constantin A, Cantagrel A, Cambon-Thomsen A, Gourraud PA (2008) New classification of HLA-DRB1 alleles in rheumatoid arthritis susceptibility: A combined analysis of worldwide samples. Arthritis Res Ther 10(1): R26. 10.1186/ar2379.
57. Delgado-Vega AM, Anaya JM (2007) Meta-analysis of HLA-DRB1 polymorphism in latin american patients with rheumatoid arthritis. Autoimmun Rev 6(6): 402–408. 10.1016/j.autrev.2006.11.004.
58. Ioannidis JP, Tarassi K, Papadopoulos IA, Voulgari PV, Boki KA, et al. (2002) Shared epitopes and rheumatoid arthritis: Disease associations in greece and meta-analysis of mediterranean european populations. Semin Arthritis Rheum 31(6): 361–370.
59. Jun KR, Choi SE, Cha CH, Oh HB, Heo YS, et al. (2007) Meta-analysis of the association between HLA-DRB1 allele and rheumatoid arthritis susceptibility in asian populations. J Korean Med Sci 22(6): 973–980.
60. Williams RC, Jacobsson LT, Knowler WC, del Puente A, Kostyu D, et al. (1995) Meta-analysis reveals association between most common class II haplotype in full-heritage native americans and rheumatoid arthritis. Hum Immunol 42(1): 90–94.
61. van der Woude D, Lie BA, Lundstrom E, Balsa A, Feitsma AL, et al. (2010) Protection against anti-citrullinated protein antibody-positive rheumatoid arthritis is predominantly associated with HLA-DRB1*1301: A meta-analysis of HLA-DRB1 associations with anti-citrullinated protein antibody-positive and anti-citrullinated protein antibody-negative rheumatoid arthritis in four european populations. Arthritis Rheum 62(5): 1236–1245. 10.1002/art.27366.
62. Fernando MM, Stevens CR, Walsh EC, De Jager PL, Goyette P, et al. (2008) Defining the role of the MHC in autoimmunity: A review and pooled analysis. PLoS Genet 4(4): e1000024. 10.1371/journal.pgen.1000024.
63. Hirschhorn JN, Lohmueller K, Byrne E, Hirschhorn K (2002) A comprehensive review of genetic association studies. Genet Med 4(2): 45–61.
64. Lohmueller KE, Pearce CL, Pike M, Lander ES, Hirschhorn JN (2003) Meta-analysis of genetic association studies supports a contribution of common variants to susceptibility to common disease. Nat Genet 33(2): 177–182.
65. Wellcome Trust Case Control Consortium (2007) Genome-wide association study of 14,000 cases of seven common diseases and 3,000 shared controls. Nature 447(7145): 661–678.
66. Plenge RM, Seielstad M, Padyukov L, Lee AT, Remmers EF, et al. (2007) TRAF1-C5 as a risk locus for rheumatoid arthritis–a genomewide study. N Engl J Med 357(12): 1199–1209. 10.1056/NEJMoa073491.
67. Plenge RM, Cotsapas C, Davies L, Price AL, de Bakker PI, et al. (2007) Two independent alleles at 6q23 associated with risk of rheumatoid arthritis. Nat Genet 39(12): 1477–1482. 10.1038/ng.2007.27.
68. Julia A, Ballina J, Canete JD, Balsa A, Tornero-Molina J, et al. (2008) Genome-wide association study of rheumatoid arthritis in the spanish population: KLF12 as a risk locus for rheumatoid arthritis susceptibility. Arthritis Rheum 58(8): 2275–2286. 10.1002/art.23623.
69. Gregersen PK, Amos CI, Lee AT, Lu Y, Remmers EF, et al. (2009) REL, encoding a member of the NF-kappaB family of transcription factors, is a newly defined risk locus for rheumatoid arthritis. Nat Genet 41(7): 820–823. 10.1038/ng.395.
70. Stahl EA, Raychaudhuri S, Remmers EF, Xie G, Eyre S, et al. (2010) Genome-wide association study meta-analysis identifies seven new rheumatoid arthritis risk loci. Nat Genet 42(6): 508–514. 10.1038/ng.582.
71. Kochi Y, Okada Y, Suzuki A, Ikari K, Terao C, et al. (2010) A regulatory variant in CCR6 is associated with rheumatoid arthritis susceptibility. Nat Genet 42(6): 515–519. 10.1038/ng.583.
72. Shimane K, Kochi Y, Horita T, Ikari K, Amano H, et al. (2010) The association of a nonsynonymous single-nucleotide polymorphism in TNFAIP3 with systemic lupus erythematosus and rheumatoid arthritis in the japanese population. Arthritis Rheum 62(2): 574–579. 10.1002/art.27190.
73. Janssens AC, Ioannidis JP, van Duijn CM, Little J, Khoury MJ, et al. (2011) Strengthening the reporting of genetic RIsk prediction studies: The GRIPS statement. PLoS Med 8(3): e1000420. 10.1371/journal.pmed.1000420.
74. Nishimura K, Sugiyama D, Kogata Y, Tsuji G, Nakazawa T, et al. (2007) Meta-analysis: Diagnostic accuracy of anti-cyclic citrullinated peptide antibody and rheumatoid factor for rheumatoid arthritis. Ann Intern Med 146(11): 797–808.
75. Peri S, Navarro JD, Amanchy R, Kristiansen TZ, Jonnalagadda CK, et al. (2003) Development of human protein reference database as an initial platform for approaching systems biology in humans. Genome Res 13(10): 2363–2371. 10.1101/gr.1680803.
76. Keshava Prasad TS, Goel R, Kandasamy K, Keerthikumar S, Kumar S, et al. (2009) Human protein reference database–2009 update. Nucleic Acids Res 37(Database issue): D767–72. 10.1093/nar/gkn892.
77. Kohler S, Bauer S, Horn D, Robinson PN (2008) Walking the interactome for prioritization of candidate disease genes. Am J Hum Genet 82(4): 949–958. 10.1016/j.ajhg.2008.02.013.
78. Sakaguchi N, Takahashi T, Hata H, Nomura T, Tagami T, et al. (2003) Altered thymic T-cell selection due to a mutation of the ZAP-70 gene causes autoimmune arthritis in mice. Nature 426(6965): 454–460. 10.1038/nature02119.
79. Barton A, Thomson W, Ke X, Eyre S, Hinks A, et al. (2008) Rheumatoid arthritis susceptibility loci at chromosomes 10p15, 12q13 and 22q13. Nat Genet 40(10): 1156–1159. 10.1038/ng.218.
80. Zhernakova A, Stahl EA, Trynka G, Raychaudhuri S, Festen EA, et al. (2011) Meta-analysis of genome-wide association studies in celiac disease and rheumatoid arthritis identifies fourteen non-HLA shared loci. PLoS Genet 7(2): e1002004. 10.1371/journal.pgen.1002004.
81. Zhernakova A, Alizadeh BZ, Bevova M, van Leeuwen MA, Coenen MJ, et al. (2007) Novel association in chromosome 4q27 region with rheumatoid arthritis and confirmation of type 1 diabetes point to a general risk locus for autoimmune diseases. Am J Hum Genet 81(6): 1284–1288. 10.1086/522037.
82. Barton A, Eyre S, Ke X, Hinks A, Bowes J, et al. (2009) Identification of AF4/FMR2 family, member 3 (AFF3) as a novel rheumatoid arthritis susceptibility locus and confirmation of two further pan-autoimmune susceptibility genes. Hum Mol Genet 18(13): 2518–2522. 10.1093/hmg/ddp177.
83. Zhernakova A, van Diemen CC, Wijmenga C (2009) Detecting shared pathogenesis from the shared genetics of immune-related diseases. Nat Rev Genet 10(1): 43–55. 10.1038/nrg2489.
84. Shen H, Cheng X, Cai K, Hu MB (2009) Detect overlapping and hierarchical community structure in networks. Physica A 388(8): 1706–1712.

85. Huang da W, Sherman BT, Lempicki RA (2009) Systematic and integrative analysis of large gene lists using DAVID bioinformatics resources. Nat Protoc 4(1): 44–57. 10.1038/nprot.2008.211.
86. Huang da W, Sherman BT, Lempicki RA (2009) Bioinformatics enrichment tools: Paths toward the comprehensive functional analysis of large gene lists. Nucleic Acids Res 37(1): 1–13. 10.1093/nar/gkn923.
87. Kochi Y, Suzuki A, Yamada R, Yamamoto K (2009) Genetics of rheumatoid arthritis: Underlying evidence of ethnic differences. J Autoimmun 32(3–4): 158–162. 10.1016/j.jaut.2009.02.020.
88. Kurreeman F, Liao K, Chibnik L, Hickey B, Stahl E, et al. (2011) Genetic basis of autoantibody positive and negative rheumatoid arthritis risk in a multi-ethnic cohort derived from electronic health records. Am J Hum Genet 88(1): 57–69. 10.1016/j.ajhg.2010.12.007.
89. Cirulli ET, Goldstein DB (2010) Uncovering the roles of rare variants in common disease through whole-genome sequencing. Nat Rev Genet 11(6): 415–425. 10.1038/nrg2779.
90. Lee-Kirsch MA, Gong M, Chowdhury D, Senenko L, Engel K, et al. (2007) Mutations in the gene encoding the 3′-5′ DNA exonuclease TREX1 are associated with systemic lupus erythematosus. Nat Genet 39(9): 1065–1067. 10.1038/ng2091.
91. Surolia I, Pirnie SP, Chellappa V, Taylor KN, Cariappa A, et al. (2010) Functionally defective germline variants of sialic acid acetylesterase in autoimmunity. Nature 466(7303): 243–247. 10.1038/nature09115.
92. Craig DW, Pearson JV, Szelinger S, Sekar A, Redman M, et al. (2008) Identification of genetic variants using bar-coded multiplexed sequencing. Nat Methods 5(10): 887–893. 10.1038/nmeth.1251.
93. Kenny EM, Cormican P, Gilks WP, Gates AS, O'Dushlaine CT, et al. (2011) Multiplex target enrichment using DNA indexing for ultra-high throughput SNP detection. DNA Res 18(1): 31–38. 10.1093/dnares/dsq029.
94. Rossin EJ, Lage K, Raychaudhuri S, Xavier RJ, Tatar D, et al. (2011) Proteins encoded in genomic regions associated with immune-mediated disease physically interact and suggest underlying biology. PLoS Genet 7(1): e1001273. 10.1371/journal.pgen.1001273.
95. Arpaia E, Shahar M, Dadi H, Cohen A, Roifman CM (1994) Defective T cell receptor signaling and CD8+ thymic selection in humans lacking zap-70 kinase. Cell 76(5): 947–958.
96. Chan AC, Kadlecek TA, Elder ME, Filipovich AH, Kuo WL, et al. (1994) ZAP-70 deficiency in an autosomal recessive form of severe combined immunodeficiency. Science 264(5165): 1599–1601.
97. Elder ME, Lin D, Clever J, Chan AC, Hope TJ, et al. (1994) Human severe combined immunodeficiency due to a defect in ZAP-70, a T cell tyrosine kinase. Science 264(5165): 1596–1599.
98. Freudenberg J, Lee HS, Han BG, Shin HD, Kang YM, et al. (2011) Genome-wide association study of rheumatoid arthritis in koreans: Population-specific loci as well as overlap with european susceptibility loci. Arthritis Rheum 63(4)): 884–893. 10.1002/art.30235; 10.1002/art.30235.
99. Terao C, Yamada R, Ohmura K, Takahashi M, Kawaguchi T, et al. (2011) The human AIRE gene at chromosome 21q22 is a genetic determinant for the predisposition to rheumatoid arthritis in japanese population. Hum Mol Genet 20(13): 2680–2685. 10.1093/hmg/ddr161.
100. Eleftherohorinou H, Hoggart CJ, Wright VJ, Levin M, Coin LJ (2011) Pathway-driven gene stability selection of two rheumatoid arthritis GWAS identifies and validates new susceptibility genes in receptor mediated signalling pathways. Hum Mol Genet 20(17): 3494–3506. 10.1093/hmg/ddr248.
101. Gunsalus KC, Ge H, Schetter AJ, Goldberg DS, Han JD, et al. (2005) Predictive models of molecular machines involved in caenorhabditis elegans early embryogenesis. Nature 436(7052): 861–865. 10.1038/nature03876.
102. Arnett FC, Edworthy SM, Bloch DA, McShane DJ, Fries JF, et al. (1988) The american rheumatism association 1987 revised criteria for the classification of rheumatoid arthritis. Arthritis Rheum 31(3): 315–324.
103. Tamiya G, Shinya M, Imanishi T, Ikuta T, Makino S, et al. (2005) Whole genome association study of rheumatoid arthritis using 27 039 microsatellites. Hum Mol Genet 14(16): 2305–2321. 10.1093/hmg/ddi234.
104. Purcell S, Neale B, Todd-Brown K, Thomas L, Ferreira MA, et al. (2007) PLINK: A tool set for whole-genome association and population-based linkage analyses. Am J Hum Genet 81(3): 559–575.
105. Janssens AC, Moonesinghe R, Yang Q, Steyerberg EW, van Duijn CM, et al. (2007) The impact of genotype frequencies on the clinical validity of genomic profiling for predicting common chronic diseases. Genet Med 9(8): 528–535. 10.1097/GIM.0b013e31812eece0.
106. Koike A, Nishida N, Inoue I, Tsuji S, Tokunaga K (2009) Genome-wide association database developed in the japanese integrated database project. J Hum Genet 54(9): 543–546. 10.1038/jhg.2009.68.
107. Yang J, Benyamin B, McEvoy BP, Gordon S, Henders AK, et al. (2010) Common SNPs explain a large proportion of the heritability for human height. Nat Genet 42(7): 565–569. 10.1038/ng.608.
108. Slatkin M (2008) Exchangeable models of complex inherited diseases. Genetics 179(4): 2253–2261. 10.1534/genetics.107.077719.
109. Lu Q, Elston RC (2008) Using the optimal receiver operating characteristic curve to design a predictive genetic test, exemplified with type 2 diabetes. Am J Hum Genet 82(3): 641–651. 10.1016/j.ajhg.2007.12.025.

THE JOURNAL OF
Obstetrics and Gynaecology Research

doi:10.1111/j.1447-0756.2011.01651.x J. Obstet. Gynaecol. Res. Vol. 38, No. 1: 137–144, January 2012

# Annexin A2 in amniotic fluid: Correlation with histological chorioamnionitis, preterm premature rupture of membranes, and subsequent preterm delivery

Fumihiko Namba[1], Shihomi Ina[3], Hiroyuki Kitajima[2], Hiroyuki Yoshio[4], Kazuya Mimura[1], Shigeru Saito[2] and Itaru Yanagihara[1]

*Departments of [1]Developmental Medicine and [2]Neonatology, Osaka Medical Center and Research Institute for Maternal and Child Health, Osaka, [3]Department of Obstetrics and Gynecology, Faculty of Medicine, University of Toyama, Toyama, and [4]Department of Neonatology, National Hospital Organization Okayama Medical Center, Okayama, Japan*

## Abstract

***Aim:*** The aim of this study was to determine whether amniotic fluid levels of annexin A2, a phospholipid-binding protein that is abundant in amnion and regulates fibrin homeostasis, are associated with histological chorioamnionitis, preterm premature rupture of the membranes, and subsequent preterm delivery.

***Materials and Methods:*** Amniotic fluid was obtained from 55 pregnant women with preterm labor and/or preterm premature rupture of the membranes before 32 weeks of gestation, and amniotic fluid levels of annexin A2 were measured with a sandwich enzyme-linked immunosorbent assay.

***Results:*** Amniotic fluid levels of annexin A2 in patients with histological chorioamnionitis was higher than that in the remainder ($P = 0.053$), whereas amniotic fluid levels of annexin A2 in patients with preterm premature rupture of the membranes was significantly higher than that in the remainder ($P = 0.002$). Amniotic levels of annexin A2 was a fair test (area under receiver–operator characteristic curve = 0.679), and amniotic fluid levels of annexin A2 > 878.2 ng/mL had a sensitivity of 68.8%, a specificity of 65.2%, a positive predictive value of 73.3%, and a negative predictive value of 60.0% for predicting delivery within 2 weeks after amniotic fluid sampling. Furthermore, the combined use of amniotic fluid cut-off levels of 878.2 ng/mL for annexin A2 and 13.3 ng/mL for interleukin-8 improved the specificity (91.3%) and the positive predictive value (89.5%).

***Conclusions:*** We identified amniotic fluid levels of annexin A2, especially in combination with amniotic fluid levels of interleukin-8, as a novel predictive marker for preterm delivery.

**Key words:** amniotic fluid, annexin A2, histological chorioamnionitis, interleukin-8, preterm premature rupture of the membranes.

## Introduction

About 40% of all infant deaths in the USA are preterm-related.[1] Preterm births account for more than 50% of long-term morbidity. Intrauterine infection has not only been recognized as a major cause of preterm labor and delivery,[2] but has also been shown to be associated with an increased risk of neurodevelopmental impairments and respiratory and gastrointestinal complications in neonates.[3,4] Because intrauterine infection is confirmed through placental pathology as histological chorioamnionitis (hCAM), early diagnosis of hCAM

Received: December 10 2010.
Accepted: March 29 2011.
Reprint request to: Dr Fumihiko Namba, Division of Neonatology, The Children's Hospital of Philadelphia Research Institute, 34th Street and Civic Center Boulevard, Philadelphia, PA 19104, USA. Email: nambaf@email.chop.edu
Present address: Fumihiko Namba, Division of Neonatology, The Children's Hospital of Philadelphia Research Institute, 34th St. and Civic Center Blvd., Philadelphia, PA 19104, USA; Hiroyuki Yoshio, Department of Pediatrics, St. Marianna University School of Medicine, 2-16-1, Sugao Miyamae-ku, Kawasaki, Kanagawa 216-8511, Japan.

clarifies the progress of infection and plays an important role in the management of patients.[5]

Microbiological cultivation is the classic 'golden standard' method for the determination of intrauterine pathogens; anaerobic bacteria, wall-less mollicutes (genus *Mycoplasma* and *Ureaplasma*), and viruses. However, the individual detection methods take time, are costly, and require experience. Recent advances in molecular biology and mass spectrometric detection enabled the rapid, highly sensitive, and specific global identification of both pathogens and host defense pathways of intrauterine infection or hCAM. The clinical biomarkers of intrauterine infections have been identified and include glucose, insulin-like growth factor-binding protein-1, cytokines, and matrix metalloproteinase (MMP) in amniotic fluid (AF).[6–9] The AF level of interleukin-8 (AF-IL-8) is an important index of hCAM and is a highly predictive marker for detecting preterm delivery before 34 weeks of gestation.[8]

The annexins are a family of calcium- and membrane-binding proteins expressed in most eukaryotic cell types.[10] Annexin A2 (AnxA2) has been implicated in membrane attachment, endocytosis, and exocytosis, which are pivotal activities for various pathogens to interact with host cells.[11–14] Furthermore, AnxA2 also functions as a modulator in immunologic clearance and for procoagulant and anticoagulant remodeling factors in vascular damage: phagocytosis,[15] von Willebrand factor secretion after histamine stimulation,[16] and fibrin clot dissolution.[17,18] It has recently become clear that certain types of dysregulation in annexin expression and activity can be correlated with human disease (e.g. the overexpression of AnxA2 in a patient with hemorrhagic form of acute promyelocytic leukemia[19] and the under-expression of annexin A5 on placental trophoblasts in the antiphospholipid syndrome[20]), which has led to the introduction of the term 'annexinopathies'.[21]

We previously identified that AnxA2 was one of the major targets of cord blood immunoglobulin M (IgM) in preterm infants with hCAM. The cord blood anti-AnxA2 IgM titer in preterm infants was correlated with the severity of hCAM.[22] This was the first report that the autoimmune response occurred in the fetal period – the fetal immune response syndrome. Because AnxA2 was expressed abundantly in amniotic epithelial cells, chorionic trophoblasts, villous trophoblasts, and villous endothelial cells,[23,24] we hypothesized that the fetal autoimmune response against AnxA2 might be triggered by the exposure of AnxA2 through inflammation and disruption around the membranes in hCAM. In this report, we constructed the sandwich enzyme-linked immunosorbent assay (ELISA) system using recombinant AnxA2[24] to measure amniotic fluid level of AnxA2 (AF-AnxA2). AF-AnxA2 seems to be correlated with hCAM and preterm premature rupture of the membranes (pPROM). The subsequent preterm delivery can be predicted by the combined assessments of AF-AnxA2 and AF-IL-8.

## Materials and Methods

### Amniotic fluid samples

After Ethics Committee approval was obtained from Toyama University, we collected AF specimens and baseline and outcome data. We studied 55 patients diagnosed with spontaneous preterm labor and/or pPROM before 32 weeks of gestation, who were managed at the Department of Obstetrics and Gynecology, Toyama University between January 2000 and November 2005. Preterm labor was defined according to the Canadian Preterm Labor Investigators group[25] as the presence of regular uterine contractions (six per 60 min documented by external tocography) or any uterine activity associated with a cervix effaced by at least 50% or dilated by 2 cm or more. To treat preterm labor, women with regular uterine contractions as defined above were treated with an intravenous infusion of the β-2 stimulant ritodrine hydrochloride (33 μg/min). When administration of ritodrine hydrochloride at the maximum dose (100 μg/min) was not effective, intravenous administration of magnesium sulfate was added (4 g/30 min), and then continued at 1–2 g/h.

After written informed consent was obtained, amniocentesis was performed in 55 cases. Amniocentesis was usually performed within a week of admission. The amniotic fluid samples were stored at –80°C until assays of ANXA2 concentrations. CAM was confirmed histologically in placental samples.

### ELISA for detection of AF-AnxA2 and AF-IL-8

AF-AnxA2 was measured using a sandwich ELISA. Mouse anti-human AnxA2 monoclonal antibody diluted at 1:2000 was coated on a 96-well microtiter plate and was incubated overnight at 4°C. After blocking with 10% fetal bovine serum at room temperature for 1 h, an AnxA2 standard (recombinant human AnxA2 expressed by *Pichia pastoris*[24]) and test samples were added into each well and incubated at 37°C for 1 h. Rabbit anti-human AnxA2 polyclonal antibody was added and incubated at 37°C for 1 h. After the plate was washed three times, peroxidase-conjugated goat anti-rabbit immunoglobulin G antibody was added

and incubated at 37°C for 1 h. AF-AnxA2 was detected with *o*-phenylenediamine. Hydrochloric acid (1M) was then added to stop the reaction. The absorbance of the solution was measured at 492 nm using a microplate spectrofluorometer. The concentration of AnxA2 in the samples was calculated from the AnxA2 standard curve. AF-IL-8 was measured with ELISA as previously reported.[26]

### Statistical analysis

The data were analyzed using the SPSS 11.0 software for Windows. Simple linear regression analysis was conducted to evaluate the correlation between AF-AnxA2 and gestational age and between AF-AnxA2 and AF-IL-8. A cohort study was conducted to compare patients who developed hCAM with the remainder of the cohort. hCAM patients and the remainder were compared with respect to baseline and outcome characteristics using appropriate parametric and non-parametric statistical tests. Differences in proportions were assessed using the $\chi^2$-test. AF-AnxA2 was compared between hCAM patients and the remainder of the cohort and between pPROM patients and the remainder using the Mann–Whitney *U*-test. Logistic regression analysis, adjusting for the potential confounding clinical factors associated with hCAM or pPROM, was conducted to evaluate the independent association of AF-AnxA2 with hCAM or pPROM. The strength of association in these models is reported as the adjusted odds ratio (OR) with the 95% confidence interval (CI). Receiver–operator characteristic (ROC) curve analysis was used to determine an optimal AF-AnxA2 cut-off point for predicting preterm delivery within 2 weeks of sampling. The $\chi^2$-test with specific cut-off levels was analyzed, and the relative risk was calculated to estimate whether patients with an AF-AnxA2 greater than the cut-off level have a risk of having preterm delivery. Each group categorized by cut-off levels of AF-AnxA2 and AF-IL-8 was compared with respect to sampling-to-delivery interval using the Mann–Whitney *U*-test. A *P*-value of <0.05 indicated significance.

## Results

### Baseline and outcome characteristics of hCAM patients and the remainder of the cohort

Fifty-five patients agreed to participate. The mean and median gestational ages at the time of sampling were 26.5 (standard deviation: 3.2) and 26.4 (range: 20.3–31.9) weeks, respectively. Of the 55 patients, there were 38 patients with hCAM (69.1%). The other 17 patients (30.9%) served as the comparison group. Baseline and outcome characteristics were compared between hCAM patients and the remaining cohort. No significant differences in maternal age, gestational ages at the time of sampling and delivery, sampling methods, number of nulliparous patients, birth weights, sampling-to-delivery intervals, and incidence of pregnancy complications were observed between hCAM patients and the remainder of the cohort (Table 1).

### AF-AnxA2

The correlation of AF-AnxA2 with gestational age is shown in Figure 1. AF-AnxA2 significantly decreased as the gestational age at the time of sampling increased between 20 and 32 weeks (simple linear regression: $\beta = -0.283$, $P = 0.036$; Fig. 1) in patients diagnosed with preterm labor and/or pPROM.

AF-AnxA2 was higher in hCAM patients than in the comparison group, but the difference was not statistically significant ($P = 0.053$; Fig. 2a). We also tested eight patients who did not have preterm labor or pPROM (mean gestational age ± standard deviation: 36.6 ± 1.6 weeks; range: 34.1–38.6 weeks) for the presence of AF-AnxA2, but it was not detected in these patients. In Figure 2a, open circles indicate patients who developed pPROM at the time of admission. We compared AF-AnxA2 between pPROM patients ($n = 16$) and non-pPROM patients ($n = 39$) in the present cohort, and AF-AnxA2 for pPROM patients was significantly higher than that for non-pPROM patients ($P = 0.002$; Fig. 2b).

Tables 2 and 3 display OR for the strength of association between hCAM or pPROM and their risk factors. Positivity for AF-AnxA2 (>878.2 ng/mL) and AF-IL-8 (>13.3 ng/mL) were significantly associated with pPROM (OR, 5.61; 95%CI, 1.38–22.88; and OR, 4.31; 95%CI, 1.18–15.81, respectively). The association between positivity for AF-AnxA2 and pPROM remained significant after adjustment for confounding factors in logistic regression analyses (OR, 6.52; 95%CI, 1.18–36.10).

### Biomarker for prediction of preterm delivery

We sought to dichotomize AF-AnxA2 to evaluate the association of elevated levels with subsequent preterm delivery within 2 weeks of sampling. ROC curve analysis of the area under the curve (68%) indicated that AF-AnxA2 is a fair test for predicting preterm delivery

**Table 1** Baseline and outcome characteristics of the cohort†

| Baseline characteristics | hCAM patients ($n = 38$) | Remaining cohort ($n = 17$) | $P$-value |
|---|---|---|---|
| Maternal age (years) | 30.1 ± 4.4 | 30.0 ± 5.6 | 0.955‡ |
| | 30 (21–38) | 28 (23–40) | 0.674§ |
| Gestational age at sampling (weeks) | 26.3 ± 3.2 | 26.8 ± 3.2 | 0.628‡ |
| | 26.3 (20.3–31.9) | 27.3 (21.1–31.6) | 0.572§ |
| Sampling | | | |
| Amniocentesis | 92% | 88% | 0.963¶ |
| Cesarean section | 8% | 12% | 0.963¶ |
| Parity | | | |
| Nulliparous | 41% | 59% | 0.338¶ |
| Pregnancy complications | | | |
| Pre-eclampsia | 0% | 6% | |
| pPROM | 37% | 12% | 0.116¶ |
| Birthweight (g) | 1444 ± 717 | 1569 ± 631 | 0.547‡ |
| | 1218 (440–2888) | 1412 (758–2670) | 0.454§ |
| Gestational age at delivery (weeks) | 29.6 ± 4.4 | 30.4 ± 4.5 | 0.515‡ |
| | 28.9 (21.9–40.3) | 31.0 (25.4–37.9) | 0.444§ |
| Sampling-to-delivery interval (days) | 22.5 ± 28.9 | 25.3 ± 28.0 | 0.742‡ |
| | 9 (0–105) | 19 (0–83) | 0.647§ |

†Data presented as mean ± standard deviation, median (range), and/or percentage. ‡Parametric $t$-test. §Non-parametric Mann–Whitney $U$-test. ¶$\chi^2$-test for categorical data. hCAM, histological chorioamnionitis; pPROM, preterm premature rupture of the membranes.

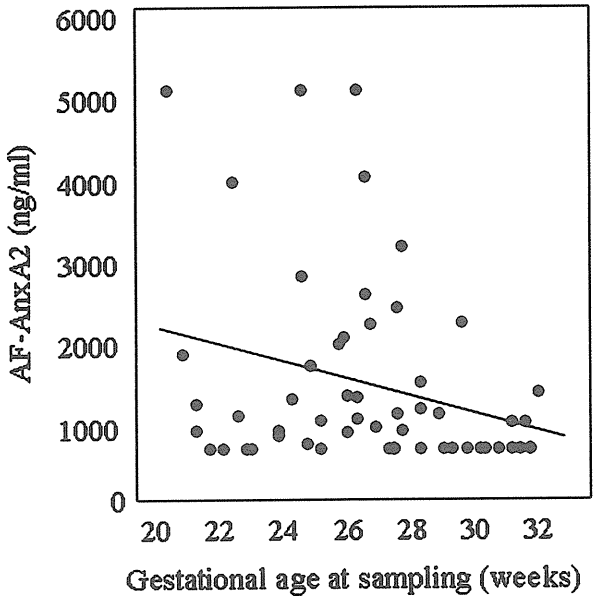


**Figure 1** Scatter plot of amniotic fluid–annexin A2 (AF-AnxA2) versus gestational age at sampling with associated regression line. AF-AnxA2 significantly decreased as the gestational age at the time of sampling increased (simple linear regression, $\beta = -0.283$, $P = 0.036$).

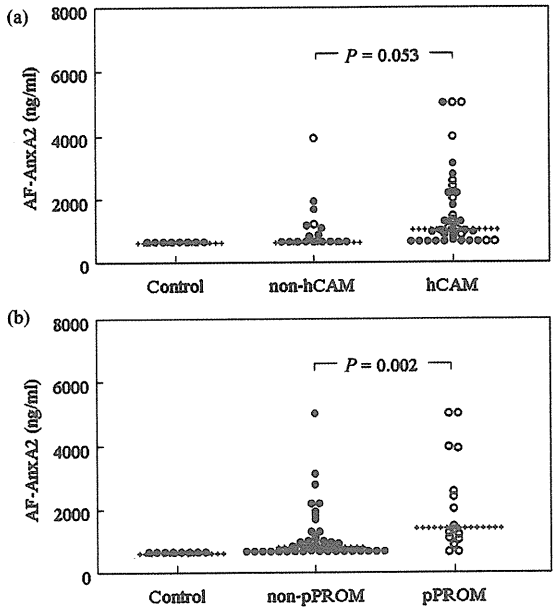


**Figure 2** Dot plot of amniotic fluid–annexin A2 (AF-AnxA2) for (a) histological chorioamnionitis (hCAM) patients versus non-hCAM patients and (b) for preterm premature rupture of the membranes (pPROM) patients versus non-pPROM patients. (a) AF-AnxA2 was higher in hCAM patients than in non-hCAM patients ($P = 0.053$). (b) AF-AnxA2 was significantly higher in pPROM patients than in non-pPROM patients ($P = 0.002$). Open circles indicate patients who developed pPROM at the time of admission.

**Table 2** Risk factors for hCAM

| | Univariate | | Multivariate | |
|---|---|---|---|---|
| | OR | 95%CI | OR | 95%CI |
| AF-AnxA2 (>878.2 ng/mL) | 3.14 | 0.95–10.37 | 2.326 | 0.62–8.74 |
| AF-IL-8 (>13.3 ng/mL) | 2.52 | 0.77–8.25 | 1.748 | 0.44–6.97 |
| Maternal age (>35 years) | 0.88 | 0.19–4.01 | 0.528 | 0.09–3.08 |
| Nulliparous | 0.48 | 0.15–1.53 | 0.579 | 0.15–2.18 |
| pPROM | 4.38 | 0.87–22.02 | 2.270 | 0.38–13.67 |

AF, amniotic fluid; AnxA2, annexin A2; CI, confidence interval; hCAM, histological chorioamnionitis; IL-8, interleukin 8; OR, odds ratio; pPROM, preterm premature rupture of the membranes.

**Table 3** Risk factors for pPROM

| | Univariate | | Multivariate | |
|---|---|---|---|---|
| | OR | 95%CI | OR | 95%CI |
| AF-AnxA2 (>878.2 ng/mL) | 5.61 | 1.38–22.88 | 6.52 | 1.18–36.10 |
| AF-IL-8 (>13.3 ng/mL) | 4.31 | 1.18–15.81 | 5.11 | 0.99–26.34 |
| Maternal age (>35 years) | 1.27 | 0.28–5.85 | 0.75 | 0.12–4.82 |
| Nulliparous | 0.70 | 0.21–2.35 | 1.24 | 0.27–5.57 |
| hCAM | 4.38 | 0.87–22.02 | 2.59 | 0.42–15.90 |

AF, amniotic fluid; AnxA2, annexin A2; CI, confidence interval; hCAM, histological chorioamnionitis; IL-8, interleukin 8; OR, odds ratio; pPROM, preterm premature rupture of the membranes.

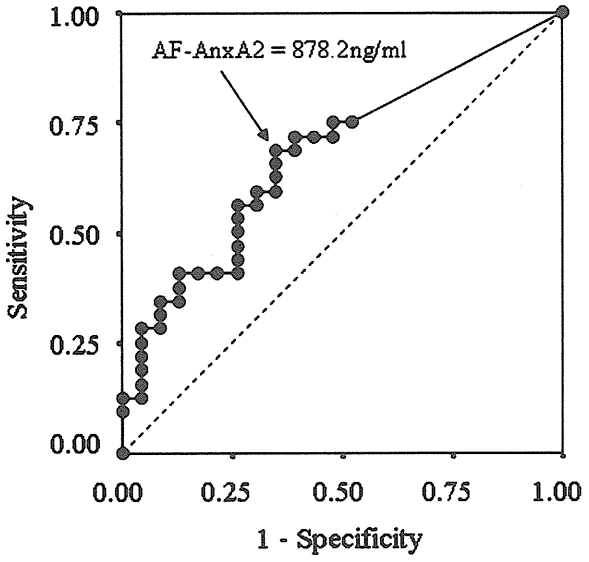


**Figure 3** Receiver–operator characteristic curve indicating the ability of amniotic fluid–annexin A2 (AF-AnxA2) to predict preterm delivery within 2 weeks of sampling. The area under the curve was 68%. At a cut-off level of 878.2 ng/mL, the sensitivity was 68.8%, the specificity was 65.2%, the positive predictive value was 73.3%, and the negative predictive value was 60.0%.

within 2 weeks (Fig. 3). An AF-AnxA2 of 878.2 ng/mL was chosen as the cut-off level, which resulted in a sensitivity of 68.8%, a specificity of 65.2%, a positive predictive value (PPV) of 73.3%, and a negative predictive value (NPV) of 60.0% (Table 4). An AF-AnxA2 > 878.2 ng/mL indicated a relative risk of 1.8 for the development of preterm delivery within 2 weeks of sampling ($\chi^2$, $P = 0.026$). In other words, patients with an AF-AnxA2 > 878.2 have a risk of developing preterm delivery within 2 weeks of sampling that is 1.8 times the risk in those with a value <878.2 (data not shown).

### Predictive value of the combination of AF-AnxA2 and AF-IL-8

We have previously reported that an AF-IL-8 > 13.3 ng/mL in pregnant women in preterm labor with intact membranes is a highly predictive marker for detecting preterm delivery before 34 weeks of gestation,[8] so we investigated the correlation between AF-AnxA2 and AL-IL-8, and whether the combination of AF-AnxA2 and AF-IL-8 was a better predictive marker for preterm delivery in patients with preterm labor or pPROM than either alone. We used an AF-AnxA2 of 878.2 ng/mL and an AF-IL-8 of 13.3 ng/mL as cut-off levels for predicting preterm delivery within 2 weeks of sampling. AF-AnxA2 was significantly correlated with AF-IL-8 (simple linear regression: $\beta = 0.407$, $P = 0.002$; Fig. 4a). The combination of AF-AnxA2 and AF-IL-8 resulted in a sensitivity of 53.1%, a specificity of 91.3%, a PPV of 89.5%, and an NPV of 58.3% (Table 4). Furthermore, sampling-to-delivery intervals were significantly shorter (median: 1.0 day) in patients with both an AF-AnxA2 > 878.2 ng/mL and an AF-IL-8 > 13.3 ng/mL (AnxA2+/IL-8+) than those in the other groups: AnxA2−/IL-8− (28.5 days), AnxA2−/IL-8+ (13.0 days), and AnxA2+/IL-8− (35.0 days) ($P < 0.01$; Fig. 4b).

## Discussion

Members of the annexin family of proteins are involved in the anti-inflammatory response.[10] Annexin A1 has

**Table 4** Diagnostic indices of AF tests in prediction of preterm delivery within 2 weeks of sampling

| Variable (cut-off value) | Sensitivity | Specificity | PPV | NPV |
|---|---|---|---|---|
| AF-AnxA2 (>878.2 ng/mL) | 68.8% (22/32) | 65.2% (15/23) | 73.3% (22/30) | 60.0% (15/25) |
| AF-IL-8 (>13.3 ng/mL) | 68.8% (22/32) | 73.9% (17/23) | 78.6% (22/28) | 63.0% (17/27) |
| AF-AnxA2 & -IL-8 | 53.1% (17/32) | 91.3% (21/23) | 89.5% (17/19) | 58.3% (21/36) |

AF, amniotic fluid; AnxA2, annexin A2; IL-8, interleukin 8; NPV, negative predictive value; PPV, positive predictive value.

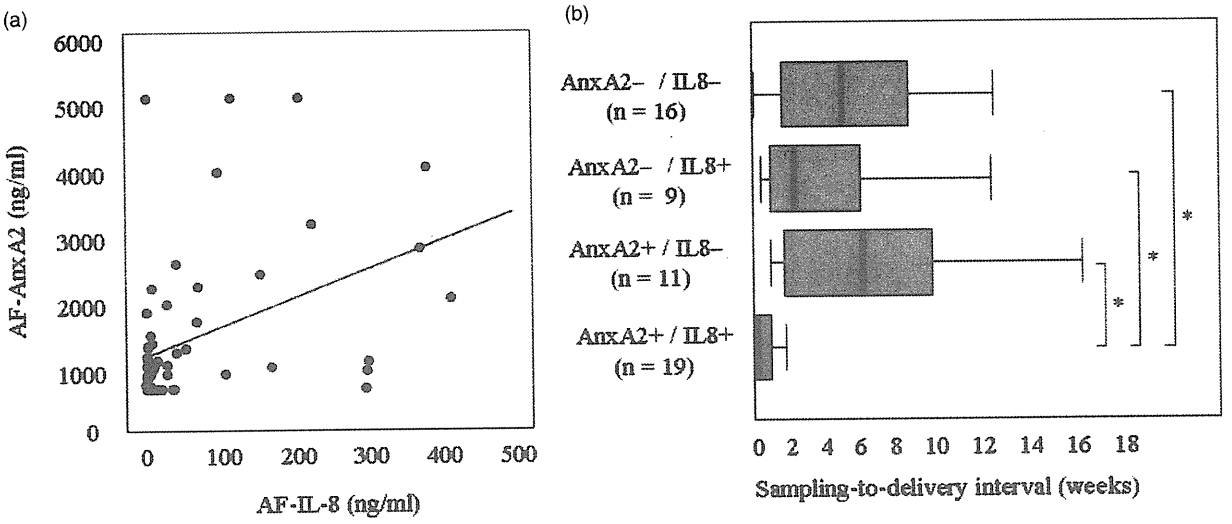


**Figure 4** (a) Correlation between amniotic fluid–annexin A2 (AF-AnxA2) and AF level of interleukin-8 (AF-IL-8). (b) Sampling-to-delivery interval in groups categorized by cut-off levels of AF-AnxA2 and AF-IL-8. (a) AF-AnxA2 correlated significantly with AF-IL-8 (simple linear regression: $\beta = 0.407$, $P = 0.002$). (b) Sampling-to-delivery intervals in patients with AF-AnxA2 > 878.2 ng/mL and AF-IL-8 > 13.3 ng/mL (AnxA2+/IL-8+) were significantly shorter (median: 1.0 day) than in the remaining cohort: AnxA2–/IL-8– (28.5 days), AnxA2–/IL-8+ (13.0 days), and AnxA2+/IL-8– (35.0 days) ($P < 0.01$).

been clearly shown to mitigate anti-inflammatory events downstream of glucocorticoid induction, as well as to inhibit arachidonic acid production via direct inhibition of phospholipase A2.[27] The AnxA2 tetramer serves as a docking protein or recognition element for bacterial and viral pathogens, such as *Pseudomonas aeruginosa*,[11] cytomegalovirus,[12] respiratory syncytial virus,[13] and macrophage-tropic HIV.[14] Furthermore, soluble AnxA2 tetramer activates human macrophages via mitogen-activated protein kinases that produce tumor necrosis factor alpha, interleukin (IL)-1 beta, and IL-6.[28] These data indicate the participation of AnxA2 in microbial clearance and establishment of inflammation. The serum level of soluble AnxA2 tetramer is low in healthy people, but is elevated in patients with an infection.[29] We previously reported that AnxA2 is a target for fetal IgM autoantibody in preterm infants, and that the anti-AnxA2 IgM titer is associated with severity of placental inflammation, that is, hCAM.[22] Therefore, in the present study, we examined whether AF-AnxA2 is a novel marker for detecting intrauterine inflammation, which is the leading cause of preterm delivery.

AF-AnxA2 in patients with preterm labor or pPROM was measurable with the sandwich ELISA developed by us. AF-AnxA2 decreased significantly as the gestational age progressed from 20 to 32 weeks. This correlation between AF-AnxA2 and gestational age seems to be implicated in the incidence of hCAM in the causative factors leading to pPROM and preterm delivery. Significantly, the earlier the gestational age at which patients present with preterm labor, the higher the frequency of intrauterine infection. At 21–24 weeks of gestation, most spontaneous births are associated with hCAM compared with about 10% at 35–36 weeks of gestation.[30]

AF-AnxA2 was compared between hCAM patients and the remaining cohort to examine the association of AF-AnxA2 with hCAM. AF-AnxA2 in hCAM patients tended to be higher than that in non-hCAM patients ($P = 0.053$). We next examined the association between AF-AnxA2 and the rupture of the chorioamniotic membrane, pPROM. AF-AnxA2 was significantly higher in patients with pPROM than in the remaining cohort ($P = 0.002$). AnxA2 protein is expressed strongly in the chorioamniotic membrane, especially in amniotic epithelial cells during gestation.[23,24] Therefore, the significant difference in AF-AnxA2 between the pPROM patients and the remaining cohort might be implicated in the expression and localization of AnxA2 in the human placenta.

ROC curve analysis was performed to evaluate the significance of AF-AnxA2 as a novel marker for predicting subsequent preterm delivery. The results showed that an AF-AnxA2 > 878.2 ng/mL was an acceptable marker for subsequent preterm delivery within 2 weeks of sampling (area under the curve: 68%). However, it was not a substantially superior, sole predictive marker for preterm delivery compared to the previously reported markers, such as AF IL-6, IL-8, glucose, and white blood cell count.[8] Thus, we next examined the importance of the combination of AF-AnxA2 and AF-IL-8 as a predictor of preterm delivery. This combination, compared with AF-AnxA2 alone, dramatically improved the specificity from 65.2 to 91.3% and the PPV from 73.3 to 89.5%. The gestational duration was shorter in patients with high AF-AnxA2 and AF-IL-8 than in those with lower levels. Moreover, 84% (16/19) of patients with high AF-AnxA2 and AF-IL-8 delivered within 1 week of sampling.

Our data indicate that AF-AnxA2 is a potential temporal biomarker for predicting preterm delivery. The secretion or release mechanism of AnxA2 from membranes into amniotic fluid is not completely clear. An increase in collagenolysis and a decrease in membrane collagen content by activation of MMP have been documented in patients with pPROM.[31] MMP activation results in increased fetal membrane apoptosis, which subsequently results in further increase in MMP activation.[32] The above findings suggest the involvement of AnxA2 secretion/release with the activation of MMP: (i) the membrane-anchored AnxA2 might be directly cleaved by MMP; and (ii) AnxA2 might be secreted concomitantly with the programmed cell death process of amniotic epithelial cells or chorionic trophoblasts.

In conclusion, we identified AF-AnxA2 as a marker for subsequent preterm delivery and pPROM, rather than for hCAM. The combination of AF-AnxA2 and AF-IL-8 may predict preterm delivery in patients with preterm labor or pPROM. Further research is clearly needed to determine the role of AnxA2 in placental inflammatory complications, and we are currently collecting data to accomplish this goal.

## Acknowledgments

This work was supported by grants-in-aid from the Ministry of Health, Labor and Welfare, Japan; the Ministry of Education, Culture, Sports, Science and Technology (MEXT), Japan; Research on Child Health and Development, Japan; and the Foundation for Mother and Child Well-being, Osaka, Japan.

## References

1. MacDorman MF, Callaghan WM, Mathews TJ, Hoyert DL, Kochanek KD. Trends in preterm-related infant mortality by race and ethnicity. United States, 1999–2004. *Int J Health Serv* 2007; **37**: 635–641.
2. Slattery MM, Morrison JJ. Preterm delivery. *Lancet* 2002; **360**: 1489–1497.
3. Willoughby RE Jr, Nelson KB. Chorioamnionitis and brain injury. *Clin Perinatol* 2002; **29**: 603–621.
4. Fujimura M, Takeuchi T, Kitajima H, Nakayama M. Chorioamnionitis and serum IgM in Wilson-Mikity syndrome. *Arch Dis Child* 1989; **64**: 1379–1383.
5. Romero R, Sirtori M, Oyarzun E *et al.* Infection and labor. V. Prevalence, microbiology, and clinical significance of intraamniotic infection in women with preterm labor and intact membranes. *Am J Obstet Gynecol* 1989; **161**: 817–824.
6. Harirah H, Donia SE, Hsu CD. Amniotic fluid matrix metalloproteinase-9 and interleukin-6 in predicting intraamniotic infection. *Obstet Gynecol* 2002; **99**: 80–84.
7. Goldenberg RL, Culhane JF. Infection as a cause of preterm birth. *Clin Perinatol* 2003; **30**: 677–700.
8. Yoneda S, Sakai M, Shiozaki A, Hidaka T, Saito S. Interleukin-8 and glucose in amniotic fluid, fetal fibronectin in vaginal secretions and preterm labor index based on clinical variables are optimal predictive markers for preterm delivery in patients with intact membranes. *J Obstet Gynaecol Res* 2007; **33**: 38–44.
9. Gravett MG, Novy MJ, Rosenfeld RG *et al.* Diagnosis of intraamniotic infection by proteomic profiling and identification of novel biomarkers. *JAMA* 2004; **292**: 462–469.
10. Gerke V, Moss SE. Annexins: from structure to function. *Physiol Rev* 2002; **82**: 331–371.
11. Kirschnek S, Adams C, Gulbins E. Annexin II is a novel receptor for Pseudomonas aeruginosa. *Biochem Biophys Res Commun* 2005; **327**: 900–906.
12. Raynor CM, Wright JF, Waisman DM, Pryzdial EL. Annexin II enhances cytomegalovirus binding and fusion to phospholipids membranes. *Biochemistry* 1999; **38**: 5089–5095.

13. Malhotra R, Ward M, Bright H *et al.* Isolation and characterisation of potential respiratory syncytial virus receptor(s) on epithelial cells. *Microbes Infect* 2003; **5**: 123–133.
14. Ma G, Greenwell-Wild T, Lei K *et al.* Secretory leukocyte protease inhibitor binds to annexin II, a cofactor for macrophage HIV-1 infection. *J Exp Med* 2004; **200**: 1337–1346.
15. Fan X, Krahling S, Smith D, Williamson P, Schlegel RA. Macrophage surface expression of annexins I and II in the phagocytosis of apoptotic lymphocytes. *Mol Biol Cell* 2004; **15**: 2863–2872.
16. Knop M, Aareskjold E, Bode G, Gerke V. Rab3D and annexin A2 play a role in regulated secretion of vWF, but not tPA, from endothelial cells. *EMBO J* 2004; **23**: 2982–2992.
17. Ling Q, Jacovina AT, Deora A *et al.* Annexin II regulates fibrin homeostasis and neoangiogenesis in vivo. *J Clin Invest* 2004; **113**: 38–48.
18. Cesarman GM, Guevara CA, Hajjar KA. An endothelial cell receptor for plasminogen/ tissue plasminogen activator (t-PA). II. Annexin II-mediated enhancement of t-PA-dependent plasminogen activation. *J Biol Chem* 1994; **269**: 21198–21203.
19. Menell JS, Cesarman GM, Jacovina AT, McLaughlin MA, Lev EA, Hajjar KA. Annexin II and bleeding in acute promyelocytic leukemia. *N Engl J Med* 1999; **340**: 994–1004.
20. Rand JH, Wu XX, Giesen P. A possible solution to the paradox of the lupus anticoagulant: antiphospholipid antibodies accelerate thrombin generation by inhibition annexin-V. *Thromb Haemost* 1999; **82**: 1376–1377.
21. Rand JH. The annexinopathies: a new category of diseases. *Biochim Biophys Acta* 2000; **1498**: 169–173.
22. Namba F, Kitajima H, Tabata A *et al.* Anti-annexin A2 IgM antibody in preterm infants: its association with chorioamnionitis. *Pediatr Res* 2006; **60**: 699–704.
23. Sun M, Liu Y, Gibb W. Distribution of annexin I and II in term human fetal membranes, decidua and placenta. *Placenta* 1996; **17**: 181–184.
24. Tabata A, Namba F, Yamada M *et al.* Expression and purification of recombinant human annexin A2 in Pichia pastoris and the utility of the expression product for detecting annexin A2 antibody. *J Biosci Bioeng* 2006; **101**: 190–197.
25. Richter R. Evaluation of success in treatment of threatening premature labor by beta mimetic drugs. *Am J Obstet Gynecol* 1977; **127**: 482–486.
26. Luo L, Ibaragi T, Maeda M *et al.* Interleukin-8 levels and granulocyte counts in cervical mucus during pregnancy. *Am J Reprod Immunol* 2000; **43**: 78–84.
27. Wu CC, Croxtall JD, Perretti M *et al.* Lipocortin 1 mediates the inhibition by dexamethasone of the induction by endotoxin of nitric oxide synthase in the rat. *Proc Natl Acad Sci USA* 1995; **92**: 3473–3477.
28. Swisher JF, Khatri U, Feldman GM. Annexin A2 is a soluble mediator of macrophage activation. *J Leukoc Biol* 2007; **82**: 1174–1184.
29. Ulvestad E, Kristoffersen EK, Jensen TS, Matre R. Identification of a soluble Fc gamma-binding molecule (annexin II) in human serum using a competitive ELISA. *APMIS* 1994; **102**: 667–673.
30. Mueller-Heubach E, Rubinstein DN, Schwarz SS. Histologic chorioamnionitis and preterm delivery in different patient populations. *Obstet Gynecol* 1990; **75**: 622–626.
31. Menon R, Fortunato SJ. The role of matrix degrading enzymes and apoptosis in rupture of membranes. *J Soc Gynecol Investig* 2004; **11**: 427–437.
32. Moore RM, Mansour JM, Redline RW, Mercer BM, Moore JJ. The physiology of fetal membrane rupture: insight gained from the determination of physical properties. *Placenta* 2006; **27**: 1037–1051.

Reproductive Sciences
http://rsx.sagepub.com/

# Ceftriaxone Preconditioning Confers Neuroprotection in Neonatal Rats Through Glutamate Transporter Upregulation

Kazuya Mimura, Takuji Tomimatsu, Kenji Minato, Otgonbaatar Jugder, Yukiko Kinugasa-Taniguchi, Takeshi Kanagawa, Masatoshi Nozaki, Itaru Yanagihara and Tadashi Kimura

*Reproductive Sciences* published online 21 June 2011
DOI: 10.1177/1933719111410710

The online version of this article can be found at:
http://rsx.sagepub.com/content/early/2011/06/14/1933719111410710

Published by:
[redacted]
http://www.sagepublications.com

On behalf of:
[redacted]
Society for Gynecologic Investigation

Reproductive Sciences
000(00) 1-9

DOI: 10.1177/1933719111410710
http://rs.sagepub.com
SAGE

# Ceftriaxone Preconditioning Confers Neuroprotection in Neonatal Rats Through Glutamate Transporter 1 Upregulation

**Kazuya Mimura, MD[1,2], Takuji Tomimatsu, MD[1], Kenji Minato, MS[1], Otgonbaatar Jugder, MD[1], Yukiko Kinugasa-Taniguchi, MD[1], Takeshi Kanagawa, MD[1], Masatoshi Nozaki, MD[2], Itaru Yanagihara, MD, PhD[2], and Tadashi Kimura, MD, PhD[1]**

**Abstract**

Objective: This study investigated the hypothesis that ceftriaxone preconditioning ameliorates brain damage in neonatal animals through glutamate transporter 1 (GLT-1) upregulation. Study design: Sprague Dawley rats were pretreated with ceftriaxone, erythromycin, minocycline, or saline for 5 consecutive days starting from postnatal day 2 (P2), and GLT-1/glutamate-aspartate transporter (GLAST) messenger RNA (mRNA) and protein levels were examined in the P7 brains. After ceftriaxone or saline preconditioning, the P7 rats underwent hypoxic-ischemic (H-I) procedure or sham operation. One week after the procedure (P14), hematoxylin-eosin staining, microtubule-associated protein 2 (MAP-2) immunostaining, and transferase-mediated deoxyuridine triphosphate nick end labeling (TUNEL) assay were used to examine neuronal damage and possible neurotoxicity. Results: Repeated ceftriaxone injections significantly increased GLT-1 mRNA and protein levels but not GLAST. Following such treatment and H-I procedure, the MAP-2-positive area increased and TUNEL-positive cells decreased. Conclusion: Antenatal ceftriaxone may help to provide neuroprotection in the immature brain and become a new prophylactic strategy to reduce neonatal encephalopathy in clinical perinatal medicine.

**Keywords**

ceftriaxone, glutamate transporter 1 (GLT-1), preconditioning, neuroprotection, neonatal rat

## Introduction

Perinatal hypoxia, which causes neonatal hypoxic-ischemic (H-I) encephalopathy (HIE), still predominates as a major cause of subsequent neurological disability in infants.[1] The response of the neonatal brain to hypoxia is vastly different from that of the adult brain.[2] Currently, no widely effective therapeutic intervention for neonatal HIE exists.

Amino acid glutamate is the major excitatory neurotransmitter in the brain and acts at postsynaptic receptors, including *N*-methyl-D-aspartate (NMDA) receptor, alpha-amino-3-hydroxy-5-methyl-4-isoxazole propionic acid receptor, and kainate receptor. Although glutamate is necessary for normal brain function and development, learning, and memory,[3] it triggers neuronal death when released in excessive amounts in response to H-I, a process known as excitotoxicity.[4] Excessively released glutamate is cleared from the extracellular space by glutamate transporters, 2 of which (glutamate transporter 1 [GLT-1] and glutamate-aspartate transporter [GLAST]) are predominantly present in glial cells of the rodent brain.[5] Glutamate transporter 1 accounts for up to 95% of total glutamate uptake in the rat brain[6-8] and is essential for maintaining low levels of extracellular glutamate[7]; thus, preventing excitotoxicity.[6,7]

It has been suggested that the immature brain is uniquely susceptible to excitotoxicity in the pathogenesis of H-I.[9] *N*-Methyl-D-aspartate receptors in the rat hippocampus are expressed at 150% to 200% of adult levels at postnatal days 6 to 14 (P6-14),[10,11] and human NMDA receptor expression peaks at 23 to 27 weeks of gestation and is even higher at term than in the adult.[12] On the other hand, GLT-1 expression in rats

[1] Department of Obstetrics and Gynecology, Osaka University Graduate School of Medicine, Suita, Osaka, Japan
[2] Department of Developmental Medicine, Osaka Medical Center and Research Institute for Maternal and Child Health, Izumi, Osaka, Japan

**Corresponding Author:**
Takuji Tomimatsu, Department of Obstetrics and Gynecology, Osaka University Graduate School of Medicine, 2-2, Yamadaoka, Suita, Osaka, 565-0871, Japan
Email: tomimatsu@gyne.med.osaka-u.ac.jp

is very low during the early postnatal period, almost reaching adult levels at approximately 3 to 4 weeks after birth.[13,14] A higher density of glutamate receptors and lower expression of GLT-1 have been considered as an explanation for the more devastating effect of excitotoxicity in the developing brain than in the adult.[9] As a result, most neonatal HIEs are clinically characterized by excessive neuronal excitation that manifests as seizures. It has been reported that NMDA receptor blockade proved to be transiently neuroprotective against H-I in neonatal rats[15,16]; however it also resulted in massive cell death by apoptosis[17] and decreased neurogenesis[18] in the immature brain. These findings suggest that glutamate controls neuronal survival and precludes NMDA receptor blockade from clinical application in perinatal medicine.

Recently, β-lactam antibiotics have been found to be the only class of agents capable of increasing GLT-1 expression by a screen of over 1000 clinically approved drugs and nutritionals.[19] Pretreatment with ceftriaxone, which efficiently penetrates the blood-brain barrier (BBB), was the most effective of several β-lactam antibiotics screened and could protect neurons from ischemic injury in adult rats.[20,21] Based on the above findings, GLT-1 upregulation by ceftriaxone may be more neuroprotective in neonates than in adults, and the immature brain thereby is a potential target for the clinical application of ceftriaxone preconditioning. Therefore, in this study, we first investigated whether ceftriaxone increases GLT-1 and GLAST expressions in the P7 rat brain, in which maturation approximates that of the term human neonate,[22] comparing it with other non-β-lactam antibiotics such as erythromycin and minocycline, which are also reportedly neuroprotective against H-I following prophylactic preconditioning in animal models.[23,24] Second, we investigated whether ceftriaxone preconditioning exerts a neuroprotective effect against H-I on the vulnerable immature brain using a model of focal H-I in the P7 rats.[25]

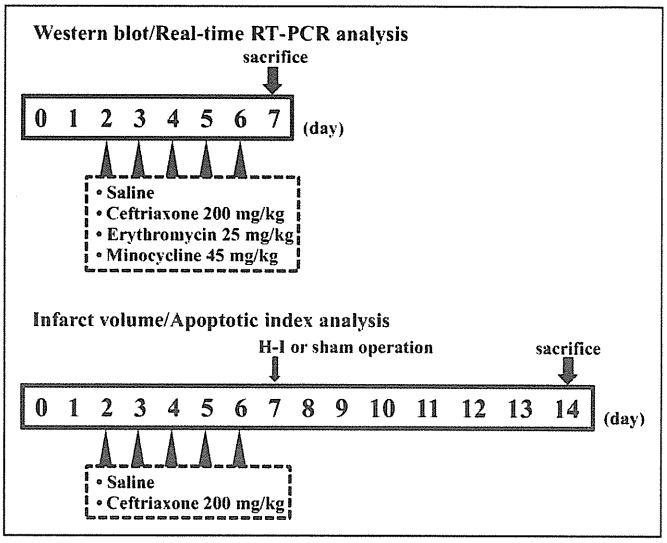


**Figure 1.** Antibiotic injections and hypoxic-ischemic (H-I) procedure or sham operation. Ceftriaxone (200 mg/kg), erythromycin (25 mg/kg), minocycline (45 mg/kg), or saline (vehicle) were administered to the pups intraperitoneally for 5 consecutive days, starting from postnatal day 2 (P2). Pups were sacrificed at P7 after the 5 days of injection for Western blot and reverse transcriptase-polymerase chain reaction (RT-PCR) analyses of glutamate transporter 1 (GLT-1)/glutamate-aspartate transporter (GLAST). The P7 pups were randomly divided into 4 groups after ceftriaxone or saline injections to analyze infarct volume and apoptosis ceftriaxone hypoxic-ischemic (H-I) group, saline H-I group, ceftriaxone sham operation group, and saline sham operation group. The sham operation group underwent the same procedures without arterial ligation or hypoxic exposure. The pups of each group were sacrificed at 7 days after the H-I injury or sham operation.

## Materials and Methods

### *Animal Model and Antibiotic Pretreatment*

This experiment was performed on Sprague-Dawley rats that were obtained from Japan SLC, Inc (Hamamatsu, Japan). The rat pups were housed with their dams and reared normally at room temperature (25°C) under a 12-hour light–dark cycle. All experimental protocols were approved by the Osaka University Animal Care and Use Committee. All efforts were made to minimize animal suffering and the number of animals used. Male and female pups weighing 9 to 12 g at P2 were uniformly divided among the study groups. We injected 200 mg/kg ceftriaxone (Chugai Pharmaceutical, Tokyo, Japan), 25 mg/kg erythromycin (Abbott, Tokyo, Japan), 45 mg/kg minocycline hydrochloride (Sigma, St. Louis, Missouri), or an equal volume of saline (vehicle) into the pups intraperitoneally once daily for 5 consecutive days, starting from P2 (Figure 1). The doses were chosen based on previous studies that observed the neuroprotective effect of antibiotics in H-I rat models.[20,23,24] For reverse transcriptase-polymerase chain reaction (RT-PCR) and Western blotting analyses, the pups were sacrificed under deep anesthesia with an overdose of sodium pentobarbital (100 mg/kg, intraperitoneally) on P7, after 5 days of pretreatment (Figure 1). The brains were rapidly removed and the hemispheric tissues were dissected (n = 8 pups per group).

### *Real-Time RT-PCR Analysis*

Tissue samples were snap frozen and homogenized for each animal, and total RNA was extracted using Isogen (Wako Pure Chemical Industries, Osaka, Japan), according to the manufacturer's instructions. After DNase I digestion (Ambion, Austin, Texas), first-strand complementary DNA (cDNA) was synthesized using PrimeScript 1st strand cDNA Synthesis Kit (Takara Bio, Shiga, Japan), according to the manufacturer's instructions. The primer sequences were as follows: GLT-1 forward 5′-CCGA GCTGGACACCATTGA-3′, reverse 5′-CGGACTGCGTCTTG GTCAT-3′; GLAST forward 5′-AATGAAGCCATCATGAGA TTGGT-3′, reverse 5′-CCCTGCGATCAAGAAGAGGAT-3′; and β-actin (internal control) forward 5′-CTACAATGAGC TGCGTGTGGC-3′, reverse 5′-CAGGTCCAGACGCAGGAT GGC-3′. Primers were purchased from Operon Biotechnologies (Tokyo, Japan). Real-time quantitative PCR was performed for

GLT-1, GLAST, and β-actin on Chromo4 (Bio-Rad, Tokyo, Japan) thermocycler, using QuantiTect SYBR Green PCR Kit (QIAGEN, Valencia, California) under the following conditions: initial denaturation at 95°C for 15 minutes followed by 35 cycles at 95°C for 20 seconds, 59°C for 30 seconds, and 72°C for 30 seconds. The generation of specific PCR products was confirmed by melting curve analysis. Both GLT1 and GLAST expressions were normalized to β-actin and analyzed with Opticon Monitor software (Bio-Rad). Polymerase chain reaction experiments were repeated twice on duplicate samples.

### Western Blot Analysis

Tissue samples were homogenized in lysis buffer (0.01 mol/L Tris [pH 7.8], 0.1 mol/L NaCl, 0.1 mmol/L ethylenediaminetetraacetic acid [EDTA], 1 mmol/L phenylmethylsulfonyl fluoride [PMSF], 2 μg/mL pepstatin, 2 μg/mL leupeptin, and 2 μg/mL chymostatin). The protein contents of the supernatants obtained after centrifugation (12 000*g*, 10 minutes) were quantified using a bicinchoninic acid (BCA) protein assay kit (Pierce, Rockford, Illinois), loaded at 20 μg/well on a 7.5% sodium dodecyl sulphate polyacrylamide gel electrophoresis (SDS-PAGE), and transferred to nitrocellulose membranes. The membranes were blocked with 5% (w/v) nonfat milk powder in phosphate-buffered saline (PBS) solution containing 0.1% Tween-20 and incubated overnight with anti-GLT-1 (1:500) and anti-GLAST (1:500) antibodies as well as with anti-β-actin (1:1000) monoclonal antibody used as the loading control (all from Santa Cruz Biotechnology, Santa Cruz, California). After washing, the membranes were incubated with a horseradish peroxidase (HRP)-conjugated secondary anti-goat/mouse antibody for 1 hour at room temperature. The blot was visualized with an enhanced chemiluminescence detection kit (Amersham, Arlington Heights, Illinois). The relative amounts of GLT-1 and GLAST were calculated from a densitometric scan. Adult rat brain extract (Santa Cruz Biotechnology) was used as a positive control.

### Induction of H-I

For the neonatal H-I experiments, the P7 pups, after 5 days of ceftriaxone or saline pretreatment were randomly divided into 4 groups: a ceftriaxone H-I group, a saline H-I group, a ceftriaxone sham operation group, and a saline sham operation group (n = 4-6 pups per group; Figure 1). The procedure for the H-I injury was derived from the model developed by Rice et al.[25] The pups were anesthetized with halothane (induction, 4.0%; maintenance, 2.0%) in room air and subsequently, the left common carotid artery was ligated surgically with a 5-0 surgical silk. After the procedure, the pups were returned to their dams and allowed to recover for 1 hour. The pups were then placed in a chamber maintained in a water bath at 37°C. The chamber was perfused with a mixture of humidified 8.0% oxygen balanced with nitrogen for 30 minutes. The sham operation group underwent the same procedure without arterial ligation or hypoxic exposure. Subsequently, the pups were returned to their dams and reared normally.

### Histological and Immunohistochemical Procedures

Pups from each group were sacrificed in the same manner as described above at 7 days after the H-I injury or sham operation. For histological analysis, the brains were perfused transcardially with 0.9% saline solution followed by 4% paraformaldehyde in 0.1 mol/L PBS at 4°C. The brains were immersed in the same fixative solution at 4°C for 24 hours, dehydrated, embedded in paraffin, and cut into 5-μm-thick coronal sections at the level of the hippocampus. Sections were deparaffinized in xylene and rehydrated in graded ethanol concentrations before staining. Slide-mounted sections were stained with hematoxylin–eosin (H-E) as well as immunohistochemically stained. Antigen retrieval for immunostaining was performed using a heating method in 10 mmol/L citrate buffer (pH 6.0) for 10 minutes. Endogenous peroxidase activity was blocked with 3% hydrogen peroxide for 10 minutes. After blocking with 5% normal goat serum, sections were incubated at room temperature for 1 hour with a 1:2000 dilution of a mouse monoclonal antibody against microtubule-associated protein 2 (MAP-2; Sigma), which is a useful marker of intact neuronal cell bodies.[26] Specimens were then incubated with biotinylated goat anti-mouse immunoglobulin G (Vector Laboratories, Burlingame, California), followed by an avidin-biotin-peroxidase solution (Vectastain ABC Elite kit; Vector Laboratories). Staining was developed with 2,3′-diaminobenzidine tetrahydrochloride in PBS containing 0.003% hydrogen peroxide.

The area of infarction was determined with the aid of a light microscope (Olympus, Tokyo, Japan) on sections that were stained with MAP-2; a loss of staining indicated infarction. A research assistant, who was unaware of the experimental protocol, analyzed the sections and measured the MAP-2-positive areas in the ipsilateral and contralateral hemispheres with Image J Imaging System Software Version 1.41 (National Institutes of Health, Bethesda, Maryland). The ratio of the MAP-2-positive area was calculated as previously described[27]:

$$\text{MAP}-2-\text{positive area ratio} = \text{MAP}-2-\text{positive area of the ipsilateral hemisphere}/\text{MAP}-2-\text{positive area of the contralateral hemisphere.}$$

### Transferase-Mediated Deoxyuridine Triphosphate Nick End Labeling Assay and Apoptotic Index

Paraformaldehyde-fixed tissues were embedded in paraffin and cut into serial sections. To assess apoptosis in the cortex, the transferase-mediated deoxyuridine triphosphate nick end labeling (TUNEL; Wako Pure Chemical Industries) assay was performed, according to the manufacturer's instructions. The tissue was counterstained with hematoxylin. Negative controls consisted of sections incubated without terminal deoxynucleotidyl transferase. A research assistant, who was unaware of the

experimental protocol, observed the sections under a light microscope using a ×40 objective lens. Three fields in the cortex were randomly selected in each section, and digital images of the TUNEL-stained (brown) and hematoxylin-stained (blue) sections were captured. Transferase-mediated deoxyuridine triphosphate nick end labeling-positive (apoptotic) and hematoxylin-stained (total) nuclei were counted using Image J Imaging System Software. The apoptotic index in each section was calculated as the percentage of the number of TUNEL-positive nuclei divided by the total number of hematoxylin-stained nuclei.

### Statistical Analysis

The analysis was conducted using GraphPad Prism (GraphPad Software, San Diego, California). All values are expressed as mean ± standard error mean (SEM). Statistical comparisons between groups were performed using 1-way analysis of variance (AVOVA) followed by Newman-Keuls post hoc test or the unpaired Student *t* test. A *P* value of <.05 was considered significant.

## Results

### Ceftriaxone Treatment Upregulated GLT-1 Expression

Both RT-PCR and Western blot analyses were performed to determine the level of GLT-1/GLAST protein and messenger RNA (mRNA) in antibiotics or saline (control)-treated rat brains. As shown in Figure 2A, treatment with ceftriaxone for 5 days (200 mg/kg per d, starting at P2) significantly increased the expression of GLT-1 mRNA (1.6-fold) but not that of GLAST at 24 hours following the treatment compared with controls. As shown in Figure 2B, treatment with ceftriaxone also increased the GLT-1 protein level but not that of GLAST compared with controls. A greater level of GLT-1/GLAST protein was observed in adult rat brain extracts considered as a positive control (Figure 2B). Densitometric analysis of immunoblots showed that the ceftriaxone treatment resulted in a significant increase (1.5-fold) in GLT-1 expression compared with controls (Figure 2C). In contrast, erythromycin and minocycline did not alter GLT-1/GLAST mRNA and protein levels (Figure 2A–C).

### Ceftriaxone Pretreatment Reduced Infarct Volume and Apoptotic Index

Cell injury in H-I brains was evaluated in the sections stained with H-E and by MAP-2 immunohistochemistry. As shown in Figure 3A, the MAP-2-positive area at 7 days after H-I revealed that ceftriaxone significantly reduced brain damage compared with that in the saline (control) H-I group. Figure 3B shows that MAP-2-positive area ratio, indicating the relative volume of intact neurons to the contralateral hemisphere, was significantly higher in the ceftriaxone H-I group than in the control. The corrected mean infarct volume in the ceftriaxone H-I group resulted in a 42% reduction compared to the control. In addition, although many TUNEL-positive nuclei appeared in the cortex at 7 days after H-I in the saline (control) H-I group (Figure 4A), a significant decrease in the number of apoptotic cells was observed in the ceftriaxone H-I group (Figure 4B).

### Glutamate Transporter I Upregulation by Ceftriaxone Did Not Induce Neurotoxicity

To examine the possible neurotoxic effect of ceftriaxone, we compared the brain sections of neonatal rats at P14 between the ceftriaxone and saline (control) sham operation groups. Ceftriaxone did not induce a loss of MAP-2 staining compared with the control (Figure 3A). In addition, TUNEL labeling was detected in very few scattered cells of the sham operated brains (Figure 4A), which corresponds to the programmed cell death that occurs during development. No significant difference in the number of apoptotic cells was observed between the ceftriaxone and control groups (Figure 4C).

## Comment

In this study, we have clearly demonstrated that ceftriaxone preconditioning reduced brain damage in the neonatal H-I model without affecting histological neurotoxicity, as measured with MAP-2 and TUNEL staining, in conjunction with an increase in GLT-1 mRNA and protein levels. Our findings suggest the neuroprotective effects of preischemic ceftriaxone through GLT-1, and the induction of GLT-1 upregulation may be in the future one of the clinically applicable strategies for preventing neonatal HIE.

Rothstein's group found that the structurally related family of β-lactam antibiotics, which include penicillin and cephalosporin antibiotics, were surprisingly effective in increasing the levels of GLT-1 protein expression but not that of GLAST in P9 rat spinal cord cultures.[19] Moreover, a 5-day ceftriaxone administration in adult rats led to a 3-fold increase in GLT-1 protein expression through increased *GLT-1* gene transcription.[20,21] Similar experiments with penicillin revealed that this antibiotic was capable of increasing the activity of GLT-1 to a lesser extent than ceftriaxone, probably because of the inability of penicillin to penetrate the BBB as effectively as ceftriaxone.[19] Non-β-lactam antibiotics, such as kanamycin and vancomycin, also had no effect on GLT-1 protein expression.[19] These findings are consistent with our results using neonatal rats.

Although the precise mechanisms of the increase in GLT-1 expression by β-lactams remain unknown, the activation of the GLT-1 genetic promoter by β-lactams has been demonstrated.[19] Furthermore, a very recent study has revealed that multiple mechanisms, including the increase of GLT-1, transcription factor, nuclear factor erythroid 2-related factor 2, and survival motor neuron protein, mediate the neuroprotective effect of ceftriaxone in a model of spinal muscular atrophy.[28] Future studies on the neuroprotective mechanisms of ceftriaxone are required.

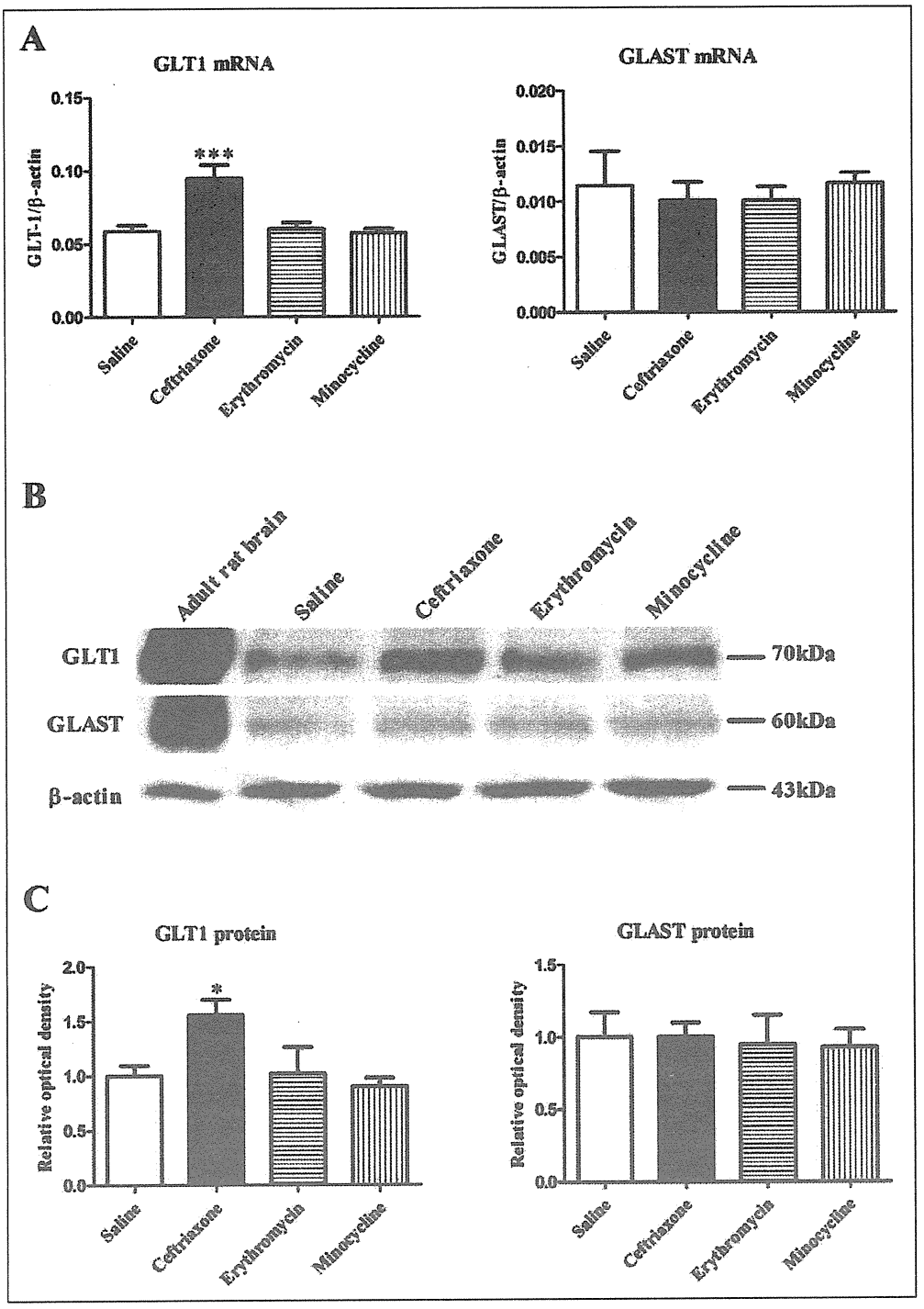


**Figure 2.** Effect of ceftriaxone on glutamate transporter 1 (GLT-1)/glutamate-aspartate transporter (GLAST) protein and messenger RNA (mRNA) expression in postnatal day 7 (P7) rats. A, Real-time reverse transcriptase-polymerase chain reaction (RT-PCR) of GLT-1 and GLAST expression after 5 days of ceftriaxone, erythromycin, minocycline, or saline (control) administration. Complementary DNA (cDNA) from the brain hemispheres was used for the RT-PCR. β-Actin was used as the internal control. All the 8 brains in each experimental group were examined. B, Western blot of GLT-1 and GLAST expression after 5 days of antibiotics or saline (control) administration. Lane 1 constitutes a positive control of adult rat brain tissue extract. Protein extracts, 20 μg, from the hemispheres were electrophoresed and blotted with GLT-1, GLAST, and β-actin (loading control) antibodies. The GLT-1 and GLAST antibodies recognized a 70-kDa GLT-1 and a 60-kDa GLAST, respectively. All the 8 brains in each experimental group were examined. Data from a representative case of each experimental group are shown. C, The relative amounts of GLT-1 and GLAST were calculated from the densitometric scan. Data are reported as mean ± SEM and represent fold-changes versus the control at 24 hours following treatment. Significant differences are indicated (* $P < .05$ vs control; *** $P < .001$ vs control). GLT-1 indicates glutamate transporter 1; GLAST, glutamate-aspartate transporter; SEM, standard error of the mean.

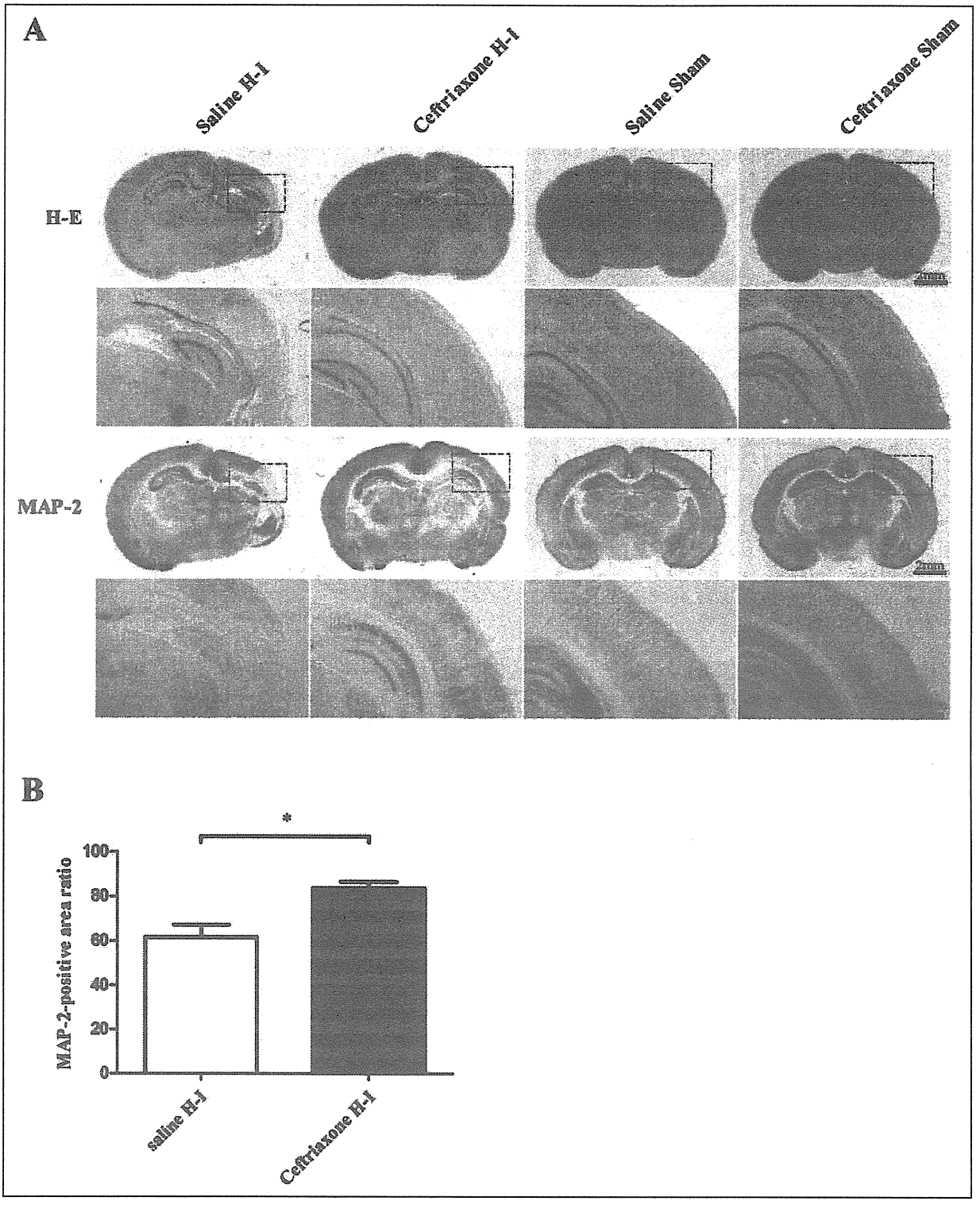


**Figure 3.** Effect of ceftriaxone on P14 rat brain damage after H-I or sham operation. A, Coronal sections were cut at the level of the hippocampus from the ceftriaxone and saline (control) groups at 7 days after H-I or sham operation. Microscopic images of H-E staining and immunostaining using microtubule-associated protein 2 (MAP-2) antibody and a higher magnification of the boxes are shown. Data were reproduced by 4 to 6 independent experiments, and the results from a representative case of each experimental group are shown. B, Pathohistological outcome was assessed by the ratio of MAP-2-positive area. Microtubule-associated protein 2-positive area ratio = MAP-2-positive area of the ipsilateral hemisphere/MAP-2-positive area of the contralateral hemisphere. Data are reported as mean ± SEM. Significant differences are indicated (* $P < .05$). P14 indicates postnatal day 14; H-I, hypoxic-ischemic; SEM, standard error of the mean.

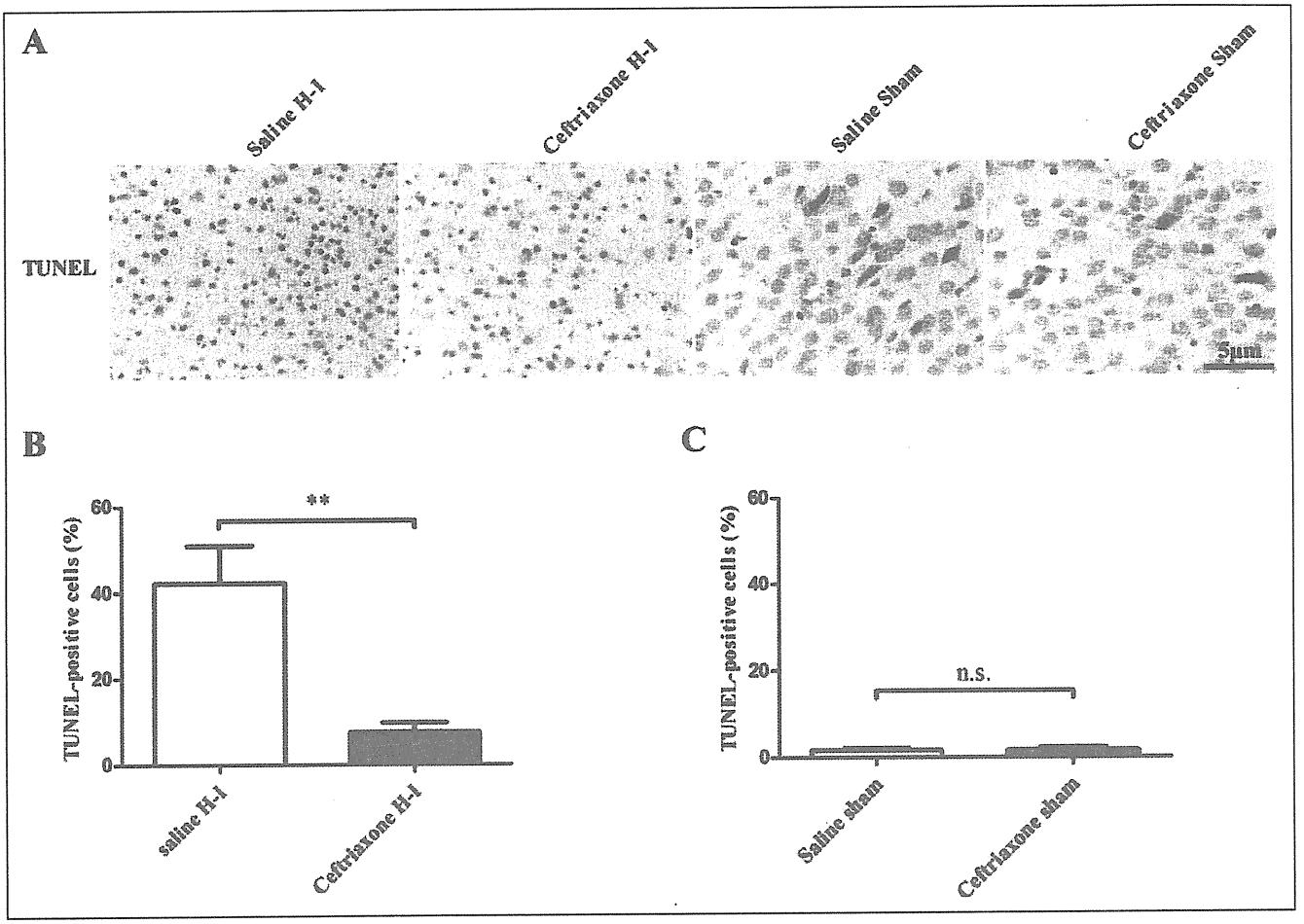


**Figure 4.** Effect of ceftriaxone pretreatment on the apoptotic index in P14 rat brain after H-I or sham operation. A, Coronal sections were cut at the level of the hippocampus from the ceftriaxone and saline (control) groups at 7 days after H-I or sham operation. Microscopic images of the transferase-mediated deoxyuridine triphosphate nick end labeling (TUNEL) stained area in the cortex using a ×40 objective lens are shown. Data were reproduced by 4 to 6 independent experiments, and the results from a representative case of each experimental group are shown. B, TUNEL-positive (apoptotic) and hematoxylin-stained (total) nuclei were counted in 3 random fields in the cortex and expressed as the average number per visual field. The apoptotic index in each section was calculated as the percentage of the number of TUNEL-positive nuclei divided by the total number of hematoxylin-stained nuclei. Data are reported as mean ± SEM. Significant differences are indicated (** $P <$ .01). n.s. indicates nonsignificant; P14, postnatal day 14; H-I, hypoxic-ischemic; SEM, standard error of the mean.

β-Lactam antibiotics, first identified with the discovery of penicillin in 1928, are now the most widely used antibiotics[29] and are considered safe to use during pregnancy.[30] To date, there are no reports of adverse neonatal neurodevelopmental effects with their use during pregnancy. The recommended human dose of ceftriaxone is 1 to 2 g once daily in adults and 50 to 100 mg/kg once daily in pediatric patients. Thus, the dose used in this study (200 mg/kg per d) was 2 to 4 times higher than the clinical dose. However, the effective concentration 50 ($EC_{50}$) for increasing GLT-1 expression by ceftriaxone in P9 rat spinal cord cultures was 3.5 μmol/L,[19] which is comparable with the human central nervous system levels that can be attained 12 hours after the treatment for meningitis (0.3-6 μmol/L).[31] Furthermore, a 2-g intravenous ceftriaxone dose of maternal administration during labor reached substantial concentrations in the umbilical cord blood within 1 hour and peaked at 4 to 8 hours; at which time, the concentrations are almost half of maternal serum concentrations.[32] The ceftriaxone concentrations achieved in fetal tissues are sufficient for therapeutic effects. Thus, the recommended clinical ceftriaxone doses are likely to be sufficient to increase GLT-1 levels in the fetus.

Although the mechanisms remain unclear, neuronal death after H-I occurs predominantly through apoptosis in the developing brain, whereas necrosis is predominating in the adult brain.[33-35] On the other hand, neurogenesis in rats occurs exceptionally in the developing brain during the first week of life.[36] Importantly, NMDA receptor blockade in the developing brain leads to massive cell death by apoptosis mainly in the cortex[17] and decreased neurogenesis in the hippocampal dentate gyrus,[18] resulting in decreased brain weight and cortical layer depth at P14.[37] To examine the possible neurotoxic effect of increasing GLT-1 expression by ceftriaxone, we analyzed apoptosis in the cortex at P14 and found no significant